Sedimentary Geology 459 (2024) 106546

Contents lists available at ScienceDirect

Sedimentary Geology

journal homepage: www.elsevier.com/locate/sedgeo

Aptian major changes in accommodation. New sedimentary evidence from the Maestrat Basin (E Iberia)

Telm Bover-Arnal [a,b,*], Joan Guimerà [b,c], Josep Anton Moreno-Bedmar [d], Carles Ferràndez-Cañadell [c], Ramon Salas [a,b]

[a] Departament de Mineralogia, Petrologia i Geologia Aplicada, Facultat de Ciències de la Terra, Universitat de Barcelona, Martí i Franquès s/n, 08028 Barcelona, Catalonia, Spain
[b] Institut de Recerca GEOMODELS, Martí i Franquès s/n, 08028 Barcelona, Catalonia, Spain
[c] Departament de Dinàmica de la Terra i de l'Oceà, Facultat de Ciències de la Terra, Universitat de Barcelona, Martí i Franquès s/n, 08028 Barcelona, Catalonia, Spain
[d] Instituto de Geología, Universidad Nacional Autónoma de México, Ciudad Universitaria, Coyoacán, 04510 México, D.F., Mexico

ARTICLE INFO

Article history:
Received 2 October 2023
Received in revised form 3 November 2023
Accepted 5 November 2023
Available online 14 November 2023

Editor: Dr. Catherine Chagué

Keywords:
Aptian
Maestrat Basin
Iberian Plate
Carbonate platform
Sea-level changes
Sequence stratigraphy

ABSTRACT

Global sea-level fluctuations with amplitudes of tens of metres and durations between 0.5 and 3 Myr are well-known oceanographic events of the Cretaceous Period. During recent years, major Cretaceous changes in accommodation recorded in different basins have been mainly interpreted as eustatically driven. Two episodes of major relative sea-level fall and rise of late early and early late Aptian age were investigated in the Maestrat Basin (E Iberian Peninsula). Previously documented in eight outcrops, these Aptian records of major changes in accommodation have now been identified in five additional localities within the basin, suggesting at least a basin-wide significance of these relative sea-level fluctuations. The records of relative sea-level fall analysed are associated with the local development of incised valleys and forced regressive wedges. Two upper lower Aptian incised valleys, which are downcutting highstand platform carbonates dominated by rudists and corals, were studied and show depths of approximately 10 and 80 m. The incision depths measured indicate amplitudes of relative sea-level variations in the order of tens of metres. During subsequent base-level rise, the lower part of these incised valleys was respectively infilled with orbitolinid limestones and high-energy carbonate deposits influenced by tides. Further evidence of major relative sea-level drop and rise during the late early Aptian includes a detached backstepping carbonate platform of reduced extension, underlain and overlain by basinal marly deposits, which flourished basinwards of a highstand platform margin. Although incised valleys or smaller-scale incisions are local features, evidence for relative declines in sea level can be identified from other evidence. For example, by the development of palaeokarst or by the presence of sharp or slightly erosive stratigraphic surfaces covered by deposits of higher energy influenced by tides, as observed in the late Aptian examples investigated herein. Comparable Aptian sedimentary features of subaerial exposure and subsequent transgressive genetic types of deposits have been observed in other basins across different tectonic plates, indicating that eustasy likely played a role in controlling accommodation changes during this stage. The discovery of new evidence for major relative Aptian sea-level fluctuations in various outcrops within the Maestrat Basin calls for further investigation in other underexplored Aptian platform carbonate successions in this basin. These investigations would contribute to a more accurate understanding of oceanographic dynamics during the Aptian Stage along the western margin of the Alpine Tethys.

1. Introduction

The Aptian Stage witnessed one of the greatest episodes of low-latitude development of carbonate platforms in the Earth's history (e.g., Skelton and Gili, 2012). Carbonate successions up to several hundred metres thick accumulated during the Aptian in warm-water settings along the margins of the Tethys (e.g., Pittet et al., 2002; Husinec et al., 2012; Pictet et al., 2015; Skelton et al., 2019; Ben Chaabane et al., 2021), as well as in the Atlantic (e.g., O'Sullivan et al., 2009; Phelps et al., 2015; Núñez-Useche et al., 2020; Loma-Villacorta et al., 2022) and Pacific (e.g., Winterer, 1991; Röhl and Ogg, 1998) regions. These vast carbonate platforms were dominated by carbonate producers such as rudist and *Chondrodonta* bivalves, nerineid gastropods,

* Corresponding author at: Departament de Mineralogia, Petrologia i Geologia Aplicada, Facultat de Ciències de la Terra, Universitat de Barcelona, Martí i Franquès s/n, 08028 Barcelona, Catalonia, Spain.
E-mail address: telm.boverarnal@ub.edu (T. Bover-Arnal).

https://doi.org/10.1016/j.sedgeo.2023.106546

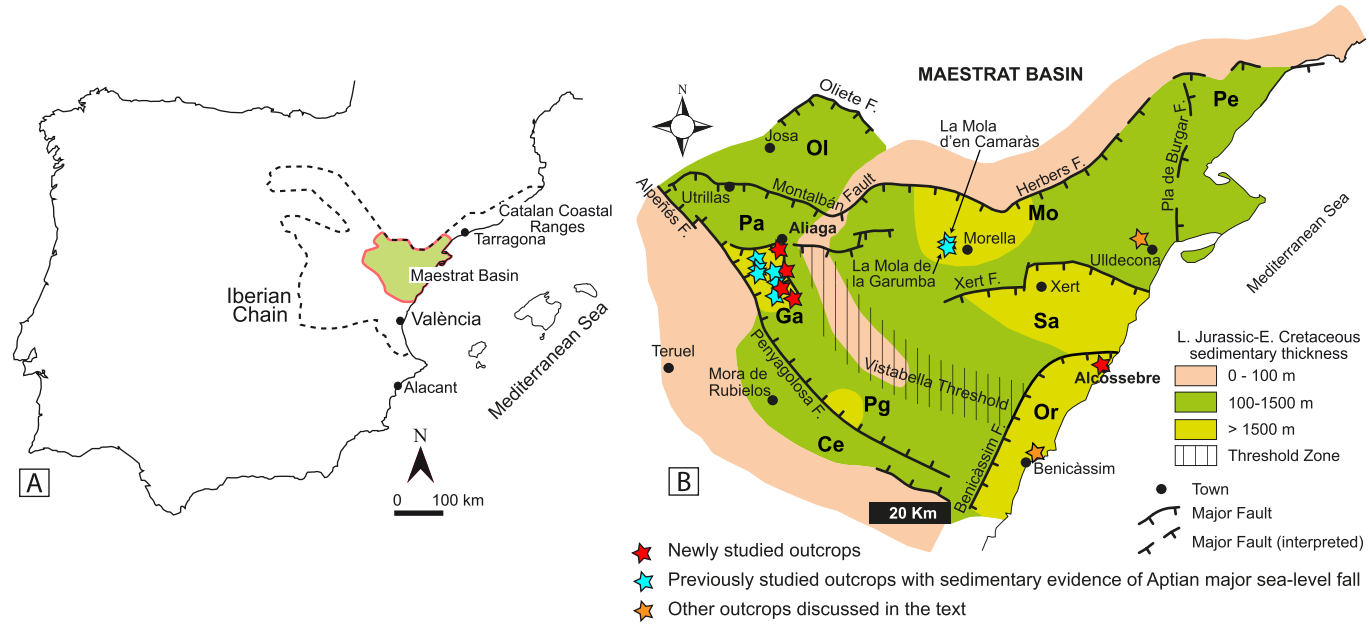
A
Iberian Chain
Catalan Coastal Ranges
Tarragona
Maestrat Basin
València
Alacant
Mediterranean Sea
N
0 100 km
B
MAESTRAT BASIN
Oliete F.
Josa
Ol
La Mola d'en Camaràs
Pe
Pla de Burgar F.
Herbers F.
Montalbán Fault
Alpenes F.
Utrillas
Pa
Aliaga
Mo
Morella
Ulldecona
La Mola de la Garumba
Xert F.
Xert
Sa
Ga
Teruel
Penyagolosa F.
Vistabella Threshold
Mora de Rubielos
Pg
Alcossebre
Or
Ce
Benicàssim F.
Benicàssim
20 Km
Mediterranean Sea
L. Jurassic-E. Cretaceous sedimentary thickness
0 - 100 m
100-1500 m
> 1500 m
Threshold Zone
Town
Major Fault
Major Fault (interpreted)
Newly studied outcrops
Previously studied outcrops with sedimentary evidence of Aptian major sea-level fall
Other outcrops discussed in the text

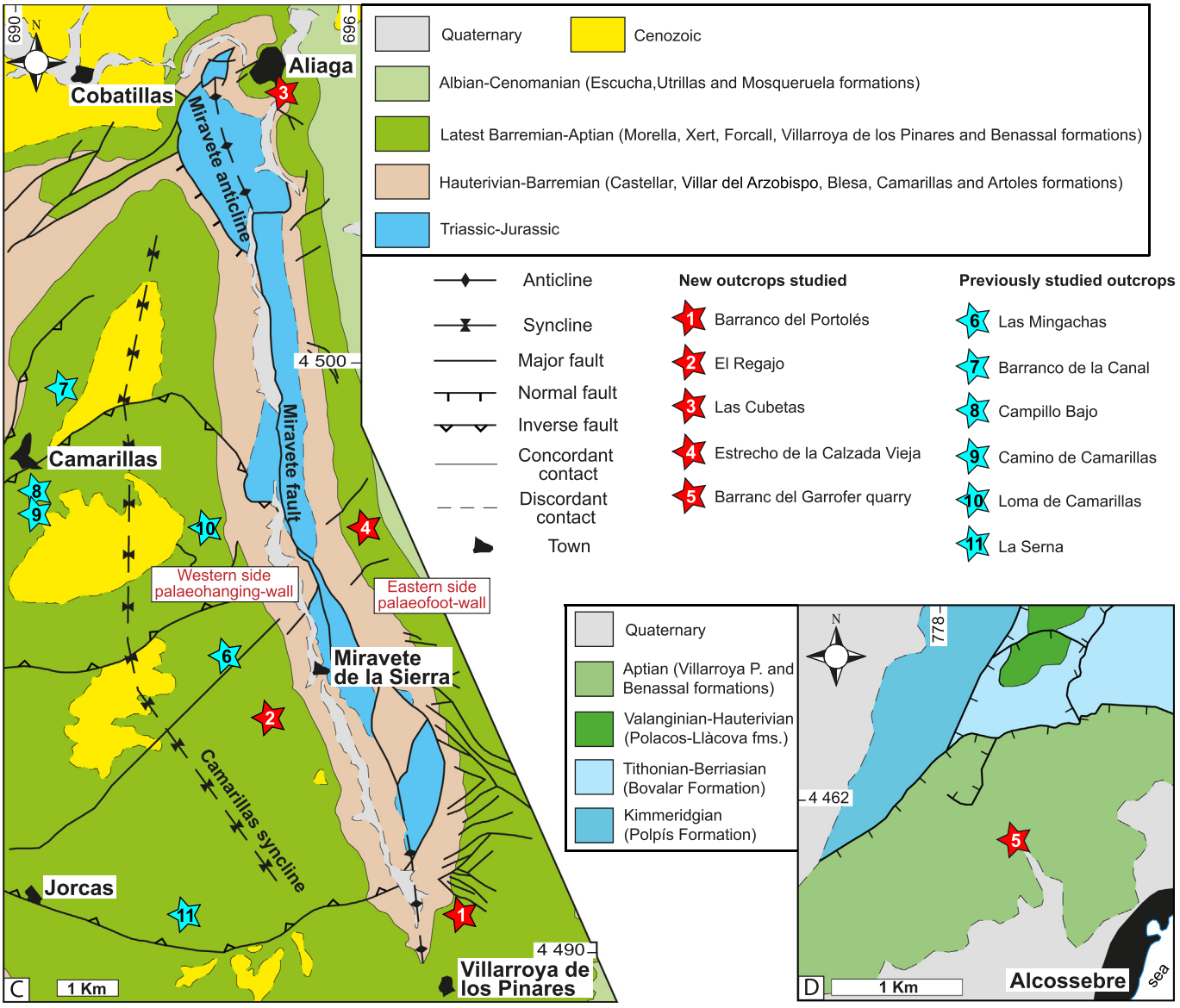
690
696
N
Cobatillas
Aliaga
Miravete anticline
Miravete fault
4 500
Camarillas
Western side palaeohanging-wall
Eastern side palaeofoot-wall
Miravete de la Sierra
Camarillas syncline
Jorcas
4 490
Villarroya de los Pinares
C
1 Km
Quaternary
Cenozoic
Albian-Cenomanian (Escucha,Utrillas and Mosqueruela formations)
Latest Barremian-Aptian (Morella, Xert, Forcall, Villarroya de los Pinares and Benassal formations)
Hauterivian-Barremian (Castellar, Villar del Arzobispo, Blesa, Camarillas and Artoles formations)
Triassic-Jurassic
Anticline
Syncline
Major fault
Normal fault
Inverse fault
Concordant contact
Discordant contact
Town
New outcrops studied
1 Barranco del Portolés
2 El Regajo
3 Las Cubetas
4 Estrecho de la Calzada Vieja
5 Barranc del Garrofer quarry
Previously studied outcrops
6 Las Mingachas
7 Barranco de la Canal
8 Campillo Bajo
9 Camino de Camarillas
10 Loma de Camarillas
11 La Serna
Quaternary
Aptian (Villarroya P. and Benassal formations)
Valanginian-Hauterivian (Polacos-Llàcova fms.)
Tithonian-Berriasian (Bovalar Formation)
Kimmeridgian (Polpís Formation)
N
778
4 462
D
1 Km
Alcossebre
sea

corals, orbitolinids, and calcareous algae (e.g., Sirna, 1999; Tomás et al., 2008; Cherchi and Schroeder, 2013; Martín-Martín et al., 2013; Ruberti et al., 2013; Pascual-Cebrian et al., 2016; Posenato et al., 2018).

Tropical to subtropical carbonate platforms are shallow-water realms and thus rises and drops in relative sea level with amplitudes of few to tens of metres can lead to their drowning or subaerial exposure, respectively. In this regard, Aptian platform carbonates accumulated in different tectonic plates show evidence of rather coeval episodes of subaerial exposure (e.g., Rameil et al., 2012; Horner et al., 2019). On the platform tops, the emersion surfaces developed as a result of Aptian relative sea-level fall, occasionally and locally show erosional incisions that allow estimates of the amplitude of Aptian relative sea-level changes (e.g., Raven et al., 2010). Basinwards, in periplatform top settings, the sedimentary records of Aptian lowering sea level include forced and/or lowstand normal regressive deposits (e.g., Bover-Arnal et al., 2009; Maurer et al., 2013).

The major events of relative sea-level drop and subsequent rise recorded during the Aptian mainly occurred in less than 3 Myr and show amplitudes that attain approximately 60 m, occasionally including larger-amplitude events (e.g., Ray et al., 2019). Eustasy, perhaps glacio-eustasy, was a main factor controlling carbonate production and sedimentation during the Aptian in the Tethys Ocean and beyond (e.g., Al-Husseini, 2013; Davies et al., 2020). In this regard, cool episodes have been recognised in Aptian records worldwide (e.g., Heimhofer et al., 2008; Rameil et al., 2012; Jaillard et al., 2019). However, indisputable geological evidence of growth and waning of large ice sheets during the Aptian that could account for such magnitudes of relative sea-level change has not been reported so far.

In the Maestrat Basin (E Iberian Plate) (Fig. 1A), two major events of fall and rise of relative sea-level during the late early and early late Aptian have been documented (e.g., Bover-Arnal et al., 2009, 2014). The Aptian events of relative sea-level change have been mainly studied in the Galve and Morella sub-basins, which correspond respectively to western and northern depocentres of the Maestrat Basin (Fig. 1B). The late early Aptian major relative sea-level fluctuation has been precisely characterised in the Galve Sub-basin (Fig. 1C) in three different contexts: i) the platform-to-basin transition area of Las Mingachas where it was recorded as a forced regressive basin-floor component and a lowstand prograding and aggrading carbonate platform that changed to retrogradation during the following transgression (see Bover-Arnal et al., 2009), ii) in the more proximal platform settings of Camarillas (Barranco de la Canal, Campillo Bajo and Camino de Camarillas outcrops) where it was recorded as incised valleys (see Bover-Arnal et al., 2009), and iii) in the isolated carbonate platform of La Serna that was also subaerially exposed and incised as a result of relative sea-level fall and shows backstepping geometries developed during subsequent relative sea-level rise (see Bover-Arnal et al., 2015). An additional outcrop showing evidence of late early Aptian lowering of relative sea level is La Mola de la Garumba (Fig. 1B), where Bover-Arnal et al. (2014) interpreted a forced regressive unit overlain by a lowstand platform. On the other hand, the early late Aptian major relative sea-level fluctuation has been studied in the deeply incised carbonate system giving rise to La Mola d'en Camaràs in the Morella Sub-basin (Fig. 1B) (see Bover-Arnal et al., 2014), and in the Loma de Camarillas site, in the Galve Sub-basin (Fig. 1C), where it was recorded as a slightly incised subaerial unconformity with development of palaeokarst (see Bover-Arnal et al., 2022).

The late early and early late Aptian relative sea-level fluctuations and their associated sedimentary records have been recently revised by Bover-Arnal et al. (2022) in the above-mentioned locations. These major sea-level events reported from eight distinct outcrops have been correlated globally, with coeval sedimentary records from other basins worldwide and thus, have been interpreted as having been mainly triggered by eustasy. Further evidence of eustatic controls on this sedimentary record is the non-angular relationship between the Aptian strata below and above of the deeply incised subaerial unconformities reported.

However, eustasy-driven falls and rises of sea level must have also had a basin-wide significance beyond the eight single outcrops mentioned above. Here we present an extended study, through basin analysis, that shows evidence of these two main Aptian sea-level changes in other sections and sub-basins of the Maestrat basin (Fig. 1C–D). New relevant outcrops showing evidence of major changes in accommodation during the Aptian are described in detail, illustrated, and interpreted. The new results in the Maestrat Basin allow us to update current knowledge about the main relative rises and falls of Aptian sea level recorded along the Central Iberian Rift System (sensu Salas et al., 2001) and the western margin of the Alpine Tethys.

2. Geological setting

The Mesozoic Maestrat Basin is located in the eastern Iberian Peninsula (Fig. 1A). It was formed as a result of two rifting cycles of Kimmeridgian to early Berriasian and Barremian to early Albian ages that were related to the spreading of the North Atlantic and the opening of the Bay of Biscay, respectively (Salas et al., 2010; García-Senz and Salas, 2011). During these rifting cycles, the Maestrat Basin was structured into nine sub-basins namely Morella, Galve, El Perelló, La Salzedella, Oliete, Las Parras, Cedramán, Orpesa and Penyagolosa (Salas et al. in Martín-Chivelet et al., 2019). In these sub-basins, Upper Jurassic–Lower Cretaceous marine and continental carbonates and siliciclastic sediments accumulated reaching thicknesses of >1.5 km in depocentral areas (Fig. 1B). Later, due to the collision between the Iberian and Euroasian plates during the Alpine orogeny, the Maestrat Basin was inverted and formed the eastern part of the Iberian Chain during the late Eocene–early Miocene (Guimerà, 1994, 2018).

The outcrops studied are located in the Galve and the Orpesa sub-basins, a western and an eastern onshore depocentres of the Maestrat Basin, respectively (Fig. 1B). In these sub-basins, the Aptian sedimentary succession is constituted by the basinal uppermost Barremian–lower Aptian marls and limestones of the Forcall Formation, which overlie the upper Barremian limestones, and locally, by sandy limestones and sandstones, of the Xert Formation (Fig. 2) (Bover-Arnal et al., 2016). The fossil record of the Forcall Formation mainly includes large-sized discoidal *Palorbitolina lenticularis*, nautiloids, and ammonoids belonging to the four lower Aptian ammonoid biozones: *Deshayesites oglanlensis*, *Deshayesites forbesi*, *Deshayesites deshayesi* and *Dufrenoyia furcata* (Bover-Arnal et al., 2010; Garcia et al., 2014). The early Aptian Oceanic Anoxic Event (OAE1a) is stratigraphically located at the upper part of the *Deshayesites forbesi* Zone within the Forcall Formation (Fig. 2) (Moreno-Bedmar et al., 2009; Cors et al., 2015). Above this latter lithostratigraphic unit, there are the upper lower Aptian platform carbonates rich in rudists, corals, *Chondrodonta* and nerineids of the Villarroya de los Pinares Formation (Canérot et al., 1982; Bover-Arnal et al., 2010).

Fig. 1. A) Geographical map of the Iberian Peninsula with the location of the Maestrat Basin in the eastern part of the Iberian Chain. B) Structural and isopach simplified map of the Late Jurassic–Early Cretaceous Maestrat Basin. The study sites in the Galve and Orpesa sub-basins, and the location of previously studied outcrops discussed in the present paper are indicated. Mo: Morella Sub-basin, Pe: El Perelló Sub-basin, Sa: La Salzedella Sub-basin, Ga: Galve Sub-basin, Ol: Oliete Sub-basin, Pa: Las Parras Sub-basin, Ce: Cedramán Sub-basin, Or: Orpesa Sub-basin, Pg: Penyagolosa Sub-basin. Modified from Salas et al. in Martín-Chivelet et al. (2019). C) Geological map modified from Canérot et al. (1979) and Gautier (1980) of the Galve Sub-basin. The outcrops analysed are indicated with red stars. The previously studied outcrops with clear physical evidence of major relative sea-level fall during the Aptian are indicated with blue stars. D) Geological setting of the Barranc del Garrofer quarry studied in the Orpesa Sub-basin. The geological map is original. Universal Transverse Mercator (UTM) Projection: Zone 30, Datum ETRS89. UTM coordinates are written in km.

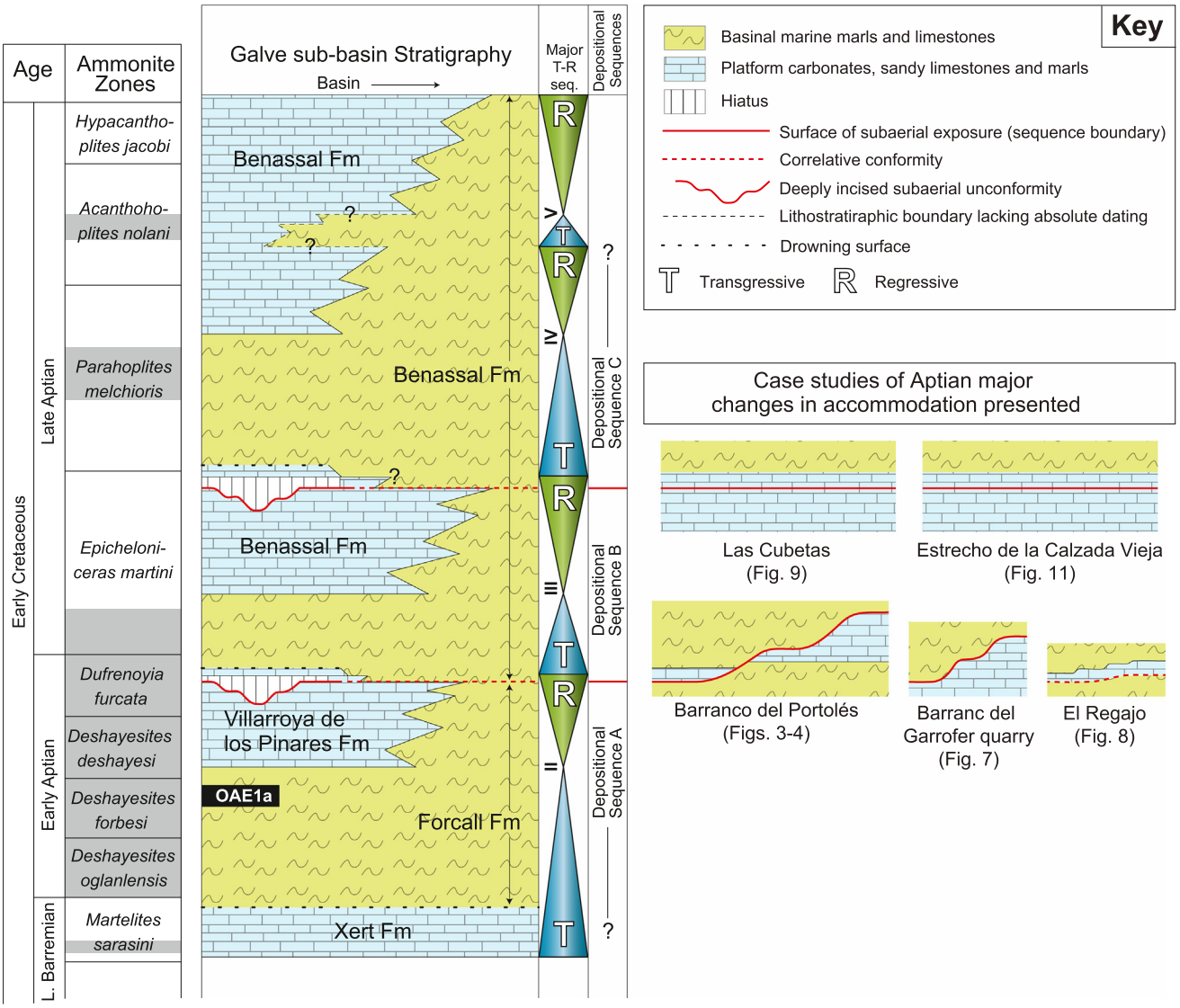

Fig. 2. Uppermost Barremian–Aptian chrono-stratigraphic scheme of the Galve Sub-basin including the major transgressive–regressive sequences interpreted by Bover-Arnal et al. (2016) and the depositional sequences interpreted in the present study and in Bover-Arnal et al. (2022). The ammonoid zonation follows Reboulet et al. (2018). The ammonite zones identified in previous biostratigraphic studies carried out in the Maestrat Basin (Moreno-Bedmar et al., 2010; Garcia et al., 2014) are highlighted in grey. Schematic and conceptual drawings of the Aptian records of major relative sea-level fall and rise studied, and their stratigraphic position are displayed on the right side of the figure.

The last Aptian lithostratigraphic unit is the Benassal Formation (Canérot et al., 1982; Salas, 1987), which spans the latest early Aptian–earliest Albian time interval (Martín-Martín et al., 2013; Bover-Arnal et al., 2022). This unit is formed by marl and limestone intervals respectively rich in gastropods and corals, and rudists, nerineids and corals (Bover-Arnal et al., 2010, 2012; Yao et al., 2020). Uppermost lower Aptian *Dufrenoyia dufrenoyi* ammonoid specimens occur at the lowermost lower marly unit of the Benassal Formation, whereas the upper Aptian *Epicheloniceras martini*, *Parahoplites melchioris* and *Acanthohoplites nolani* ammonite zones are recorded within the lower, middle, and upper marly parts of the Benassal Formation, respectively (Fig. 2) (Bover-Arnal et al., 2016). The late early and early late Aptian major events of fall and rise of relative sea-level studied in this paper are recorded at the upper part of the Villarroya de los Pinares Formation, and at the upper part of the first limestone interval of the Benassal Formation (Fig. 2).

The uppermost Barremian–Aptian succession of the Maestrat Basin was arranged into four transgressive–regressive sequences by Bover-Arnal et al. (2016) and into three depositional sequences, A, B and C, by Bover-Arnal et al. (2022). The stratigraphic intervals studied herein comprise the late early and early late Aptian sequence boundaries that respectively bound depositional sequences A and B, and B and C (Fig. 2).

3. Study sites and methods

The sedimentary records of late early Aptian major relative sea-level fall and rise were analysed in two outcrops of the Galve Sub-basin, namely Barranco del Portolés (latitude: 40.54118, longitude: −0.66593) and El Regajo (latitude: 40.57053, longitude: −0.70899), and in the Barranc del Garrofer quarry (latitude: 40.25945, longitude: 0.27575) in the Orpesa Sub-basin (Fig. 1B). The Barranc del Garrofer quarry is located to the North-East of Alcossebre (Comarca of El Baix Maestrat) (Fig. 1D), whereas the Barranco del Portolés and El Regajo study sites are respectively located near the towns of Villarroya de los Pinares and Miravete de la Sierra (Comarca of El Maestrazgo) (Fig. 1C).

The lower upper Aptian succession recording a major episode of relative sea-level swing was studied in the Galve Sub-basin (Fig. 1B), in the outcrops of Las Cubetas (latitude: 40.66920, longitude: −0.70199) and the Estrecho de la Calzada Vieja (latitude: 40.59894, longitude: −0.68517) (Fig. 1C). These study sites are located respectively near the

towns of Aliaga (Comarca of Cuencas Mineras) and Miravete de la Sierra (Comarca of El Maestrazgo).

The Aptian rocks of Las Cubetas, the Estrecho de la Calzada and the Barranco del Portolés were previously studied by Vennin and Aurell (2001), Bover-Arnal et al. (2010) and Embry et al. (2010). Vennin and Aurell (2001) originally named the sections of Las Cubetas, Barranco de la Calzada Vieja and Barranco del Portolés as Aliaga, Miravete and Portolés, respectively. Peropadre Medina (2012) also studied the Aptian successions of Las Cubetas and the Barranco del Portolés, whereas Bonin et al. (2016) further analysed the Aptian sedimentary record of Las Cubetas in Aliaga. For this study, only subaerial unconformities of late early and early late Aptian age and their superjacent and subjacent beds have been revisited for further analysis. The outcrops of the Barranc del Garrofer quarry in the Orpesa Sub-basin (Fig. 1B, D), and El Regajo in the Galve Sub-basin (Fig. 1B, C), are described here for the first time.

Sedimentary facies and surfaces with sequence-stratigraphic significance including subaerial unconformities, transgressive surfaces and maximum flooding surfaces were mapped on panoramic images and close-up photographs of the outcrops. Three stratigraphic logs 10, 10 and 13 m thick were measured and analysed bed-by-bed in the Barranco del Portolés, Las Cubetas and the Estrecho de la Calzada Vieja, respectively (Fig. 1C). A total of 31 thin sections were made from 24 samples collected in the five outcrops studied. The thin sections were analysed under a petrographic microscope to determine skeletal and non-skeletal components, as well as rock textures, which follow the classifications of Dunham (1962) and Embry and Klovan (1971). The sequence-stratigraphic terminology used in this study is taken from Catuneanu et al. (2009).

4. Results and interpretations

4.1. Late early Aptian examples of major relative sea-level change

4.1.1. Barranco del Portolés

4.1.1.1. Sedimentary and palaeontological description. In the Barranco del Portolés (Figs. 1C, 3), upper Barremian *Palorbitolina lenticularis*-rich floatstone and rudstone limestones of the Xert Formation are overlain by the lower Aptian basinal marls and limestones with ammonites, nautiloids, *P. lenticularis*, *Praeorbitolina cormyi* and *Lithocodium aggregatum* of the Forcall Formation. At the southern side of the creek, above the Forcall Formation, are aggrading platform carbonates of the Villarroya de los Pinares Formation (Fig. 4A–C). The limestones of the Villarroya de los Pinares Formation exhibit floatstone and rudstone textures and contain macrofossils such as corals, gastropods, *Chondrodonta* and the rudists *Toucasia carinata*, *Polyconites hadriani* and *Monopleura* sp.

These limestones with rudists and corals are truncated by a deeply incising erosional surface with ramps and flats that also affects the uppermost part of the Forcall Formation (Figs. 3, 4). The depth of the incision is ≥80 m and its width ≥1,8 km. At the deepest part of the incision palaeotopographic relief, an orangish limestone succession belonging to the Villarroya de los Pinares Formation is underlain and overlain by marl deposits of the Forcall and Benassal formations, respectively (Fig. 4A–B, D). This limestone succession was logged nearby the creek, in the lower part of its northern side ridge (Figs. 4D, 5).

At the northern side of the Barranco del Portolés (Fig. 4A–B, D), the Villarroya de los Pinares Formation starts with 2 m of cross-bedded grainstone textures (Fig. 5) dominated by oysters (Fig. 6A). The cross-bedded orangish limestones locally exhibit bidirectional sedimentary structures (Fig. 6B) and a basal conglomerate deposit (Fig. 5). Besides oysters, *P. lenticularis*, *Orbitolinopsis*, miliolids, other benthic foraminifera, encrusting foraminifera, serpulids, and fragments of other molluscs, echinoids, *Permocalculus* and corals, also occur. Non-skeletal components include intraclasts, peloids and silt-sized quartz grains (Fig. 5). Above the grainstone interval, a 2 m-thick conglomerate with rounded flattened pebble-sized clast occurs (Figs. 5, 6C). The matrix of the conglomerate deposit exhibits a packstone texture rich in oysters. Other common to rare components include intraclasts, peloids, *P. lenticularis*, other benthic foraminifera, encrusting foraminifera, and fragments of other molluscs, bryozoans, echinoids and *Permocalculus* (Fig. 5). The pebbles exhibit a packstone texture with abundant *P. lenticularis* and *Gastrochaenolites* with valves of lithophagid bivalves preserved inside the boring (Fig. 6D). Other common components identified in the rock pebbles are oysters, other fragments of molluscs, fragments of echinoids and bryozoans, miliolids, other benthic foraminifera, encrusting foraminifera, peloids and silt-sized quartz particles. Succeeding the conglomerate is a succession of 4 m-thick cross-bedded grainstone limestones dominated by oysters (Fig. 5). Other common to rare components are orbitolinids, miliolids, other benthic foraminifera, encrusting foraminifera, serpulids, and fragments of other molluscs, crustaceans, bryozoans, echinoids, *Permocalculus* and corals, as well as peloids and intraclasts (Fig. 5).

The lower part of the Benassal Formation in the Barranco del Portolés consists of a marly interval (Figs. 4, 5), which also includes interbedded marly-limestones and limestones, containing *Mesorbitolina parva*, echinoids, oysters, other bivalves, gastropods and very rare ammonites. Above, platform carbonates (Fig. 4A–C) with rudists, gastropods, corals and miliolids occur.

4.1.1.2. Depositional and sequence-stratigraphic interpretation. After the deposition of the lower Aptian transgressive basinal marls of the Forcall Formation, an upper lower Aptian carbonate platform with rudists and corals flourished during a highstand stage of relative sea level (Fig. 4A–B). In the Barranco del Portolés, these platform carbonates (Villarroya de los Pinares Formation; Depositional Sequence A) show an aggrading pattern (Fig. 4C). On the other hand, in the platform-to-basin transition area of Las Mingachas (Fig. 1C) (see Bover-Arnal et al., 2009, 2022), the oldest and coeval carbonate platform belonging to the Villarroya de los Pinares Formation starts with aggradation and ends with progradation, which is indicative of a highstand normal regression (e.g., Catuneanu et al., 2009).

As a result of relative sea-level fall, in the Barranco del Portolés site, the highstand normal regressive carbonates of the Villarroya de los Pinares Formation were subaerially exposed and eroded (Figs. 3, 4A–C). The erosional profile generated, which is ≥80 m deep and ≥1,8 km wide, is in accordance with an incised valley. The flat and ramp geometry of the subaerial unconformity is interpreted as the result of alternating and successive phases of stream-cutting erosion and lateral planation (see Bover-Arnal et al., 2014, 2022).

During subsequent relative sea-level rise, a transgressive surface was superposed onto the subaerial unconformity giving rise to a composite sequence boundary (Figs. 4–5). The lowermost part of the palaeovalley was infilled with uppermost lower Aptian cross-bedded grainstone textures rich in oysters (Figs. 5, 6A–B) with interbedded conglomerate deposits that belong to the Villarroya de los Pinares Formation (Figs. 5, 6C). The clasts of the conglomerate deposits, which exhibit *Gastrochaenolites* borings and are made up of packstone textures with *P. lenticularis* (Fig. 6D), were likely eroded from the upper part of the Forcall Formation and redeposited under littoral conditions within the palaeovalley. This is confirmed by the packstone matrix surrounding the pebbles which is rich in shallow-marine fossils such as *Permocalculus* (Figs. 5, 6C).

Incised valleys are commonly back-filled during lowstand and/or transgressive stages of relative sea level. However, distinctive prograding–aggrading or retrograding stacking patterns that could differentiate between lowstand and transgressive types of deposits were not observed in the lower part of the palaeovalley infilling analysed. Generally, lowstand incised-valley infills correspond to fluvial deposits (e.g., McClung et al., 2016; Ximenes Neto et al., 2021), whilst estuarine to marine infillings are commonly interpreted as transgressive deposits, as reported from other Cretaceous and more recent examples

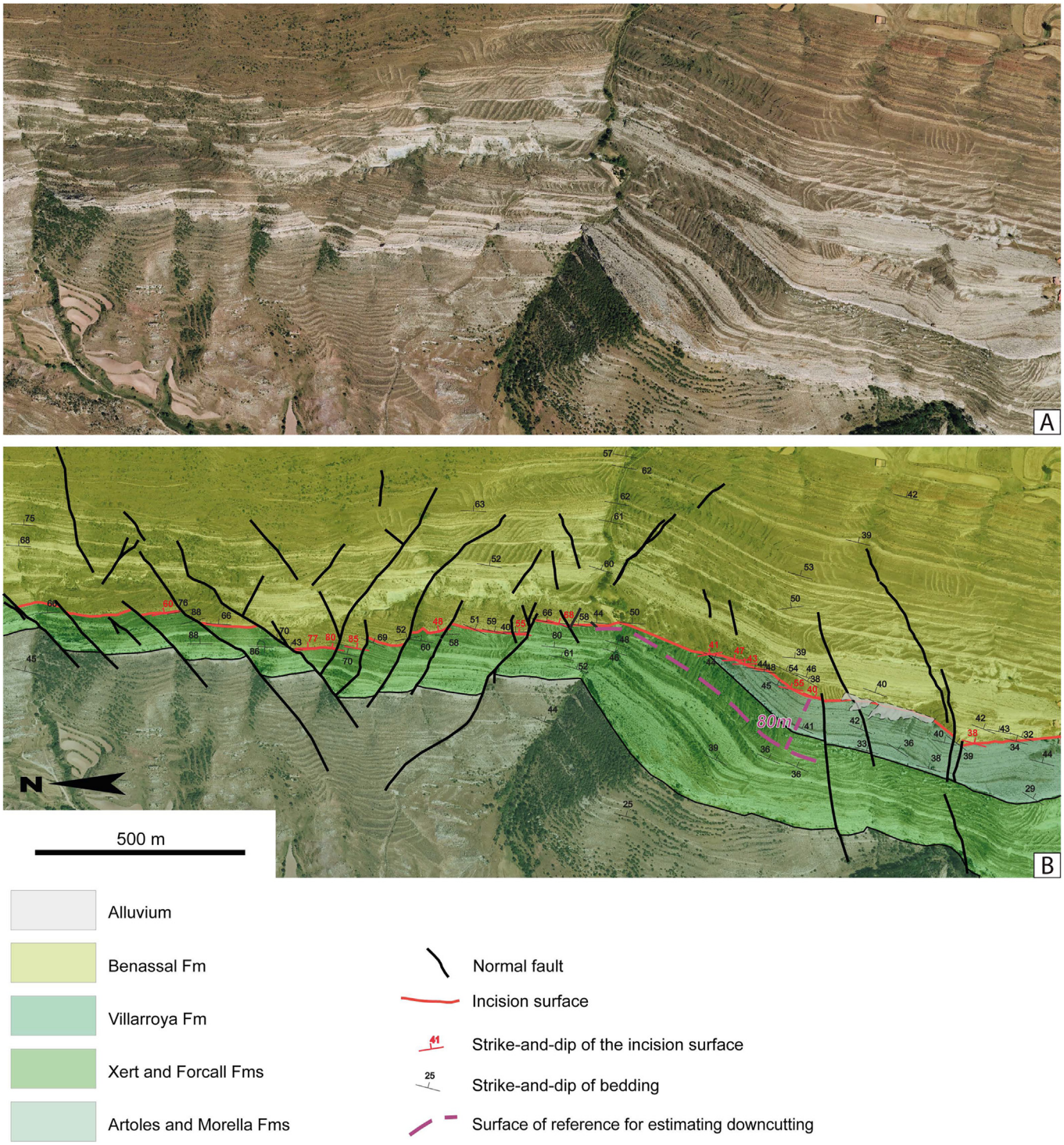

Fig. 3. Barranco del Portolés. A) Aerial view of the upper lower Aptian incised valley cutting down the Villarroya de los Pinares Formation and the upper part of the Forcall Formation. B) Interpretation of A. Note that the incised valley exhibits a minimum depth of around 80 m.

(e.g., Dalrymple et al., 1992; Chaumillon et al., 2008; Raven et al., 2010). Therefore, although it is possible that at least part of the high-energy valley-fill described was formed during a lowstand normal regression, we interpret it as early transgressive deposits of Depositional Sequence B (Figs. 4A–B, D, 5).

During this early transgressive stage, the carbonate factory supplying sediment accumulated within the palaeovalley was drowned, and subsequently buried by the basinal marls of the Benassal Formation (Figs. 4A–B, D, 5). This late transgressive marly unit, which is latest early–late Aptian in age, back-filled the upper part of the incised valley (Fig. 4A–C). Above this marly interval, platform carbonates with rudists and corals, also belonging to the Benassal Formation, are interpreted as aggrading highstand normal regressive deposits of Depositional Sequence B (Fig. 4).

4.1.2. Barranc del Garrofer quarry

4.1.2.1. Sedimentary and palaeontological description. The succession commences with well-bedded and massive decimetre- to metre-thick limestones of the top of the upper lower Aptian Villarroya de los Pinares

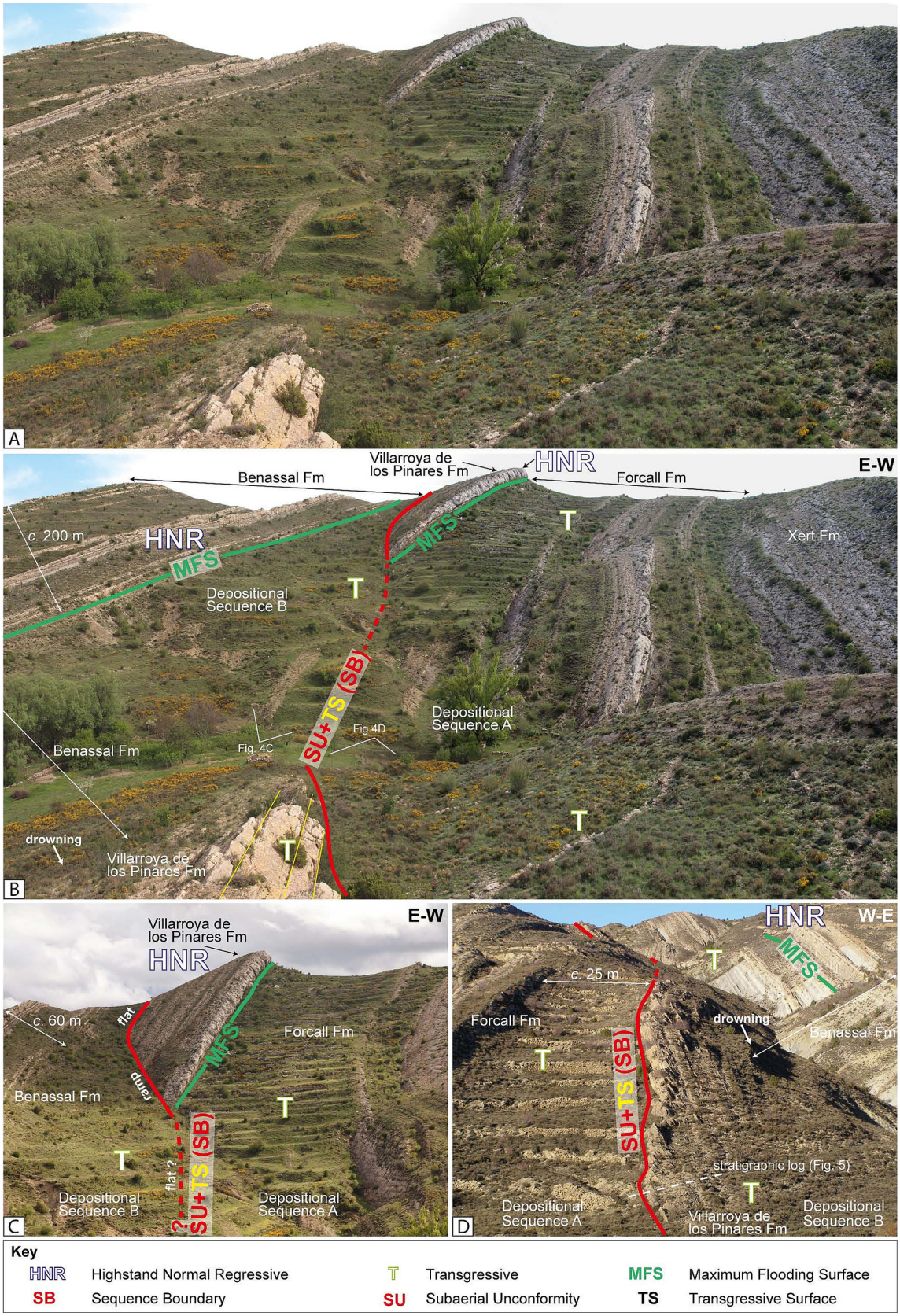

Fig. 4. Barranco del Portolés. A) Panoramic view of the upper lower Aptian incised valley. B) Interpretation of A including the lithostratigraphic units, the sequence stratigraphic framework, and the location of C–D. Note the deeply incised subaerial unconformity (SU) cutting downwards into the highstand platform carbonates of the Villarroya de los Pinares Formation and the uppermost part of the Forcall Formation. Note also how the transgressive surface is superposed onto the subaerial unconformity giving rise to a composite sequence boundary, and how this sequence boundary is onlapped by early transgressive valley-fill limestones, which also belong to the Villarroya de los Pinares Formation. C) Outcrop view of the deeply incised highstand normal regressive limestones of the Villarroya de los Pinares Formation including the sequence-stratigraphic interpretation and the lithostratigraphic units. See B for location. D) Outcrop view of the early transgressive tidal-influenced back-fill deposits including the sequence-stratigraphic interpretation, the lithostratigraphic units and the stratigraphic log shown in Fig. 5. See B for location.

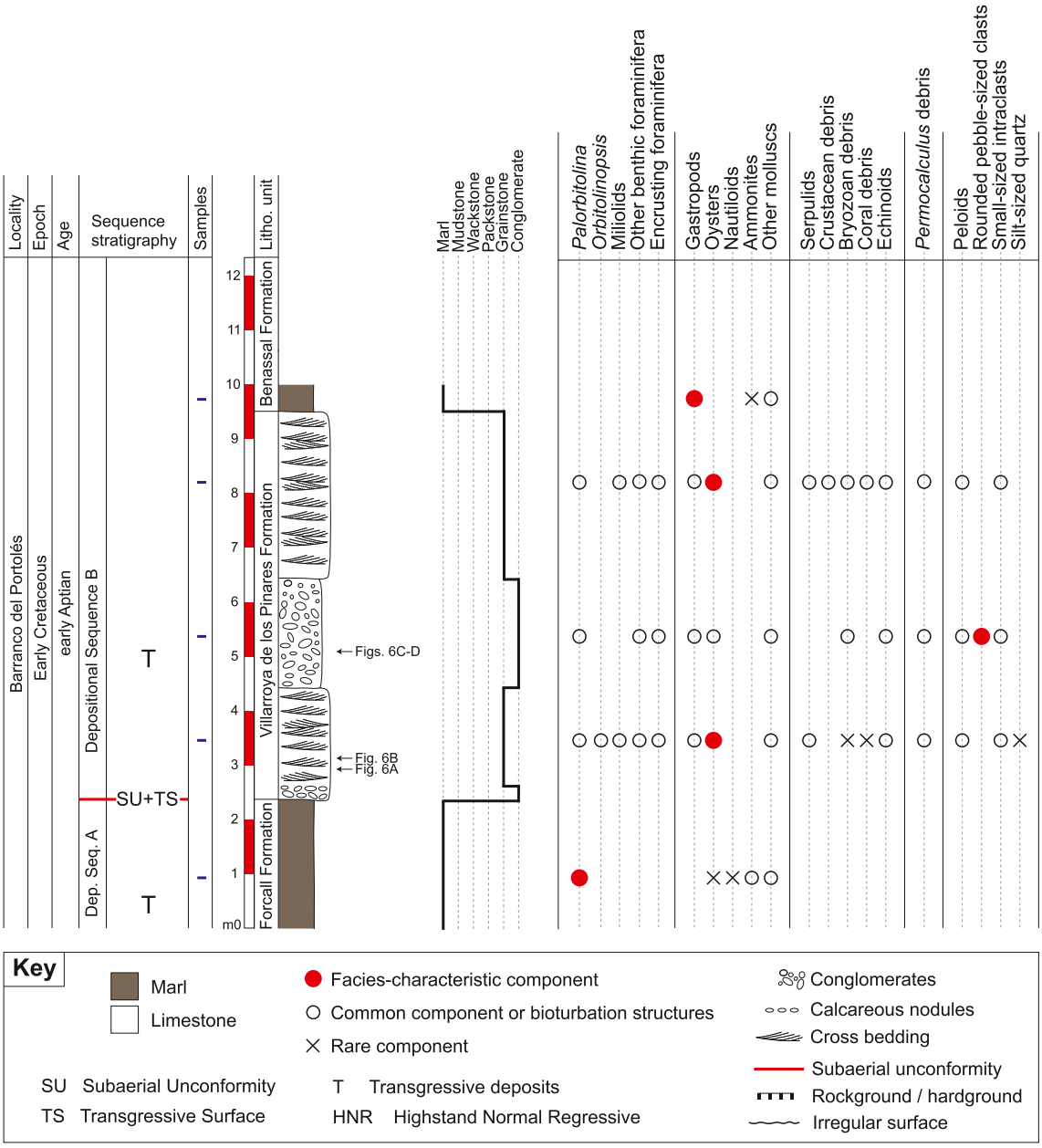

Fig. 5. Sedimentary log of the upper lower Aptian early transgressive valley-fill limestones cropping out in the Barranco del Portolés. The stratigraphic section displays the sequence-stratigraphy analysis, the stratigraphic position of the samples collected, the lithostratigraphic units, the lithology, the main petrographic components present and qualitative abundances, the bedding, the textures, the sedimentary features, the location of photographs in Fig. 6, and the stratigraphic position of the skeletal and non-skeletal components identified. See Fig. 4D for location of the section.

Formation (Fig. 7A–C). The limestones mainly exhibit floatstone and rudstone textures dominated by rudist bivalves that locally form biostromes (Fig. 7C), and packstone textures rich in miliolids. Genera and species of rudists determined include *Polyconites hadriani* (see Skelton et al., 2010) and *Toucasia*. Other common components identified are other undetermined bivalves, fragments of gastropods, *Permocalculus* and echinoids, other small benthic foraminifera, *Bacinella*-like microfabrics (see Schlagintweit and Bover-Arnal, 2013), sponge spicules and peloids.

Capping the Villarroya de los Pinares Formation is an incised subaerial unconformity of late early Aptian age displaying a flat-ramp geometry (Fig. 7A–B). The portion of the erosional incision outcropping exhibits a depth of c. 10 m. Above, marls and decimetre-thick limestones of the lowermost part of the terminal lower upper Aptian Benassal Formation onlap the ramps and overlie the flats of this erosional surface carved into the Villarroya de los Pinares Formation (Fig. 7A–B). The limestones at the base of the Benassal Formation are mainly grainstone textures with abundant large-sized discoidal orbitolinids (Fig. 7D). Other common skeletal and non-skeletal components are unidentified benthic foraminifera, fragments of *Permocalculus*, bryozoans, bivalves, gastropods, echinoids, serpulids, peloids and intraclasts (Fig. 7D). The upper part of the Benassal Formation is characterised by thicker and massive limestone beds rich in large *Chondrodonta* and rudist bivalves.

4.1.2.2. Depositional and sequence-stratigraphic interpretation. The upper part of the Villarroya de los Pinares Formation is made up of metre-thick massive platform top carbonates (Fig. 7A–B), including *Polyconites* biostromes (Fig. 7C), which are characteristic of aggrading platform-top settings during highstand stages of relative sea level (e.g., Bover-Arnal et al., 2009, 2022). Accordingly, the Villarroya de los Pinares

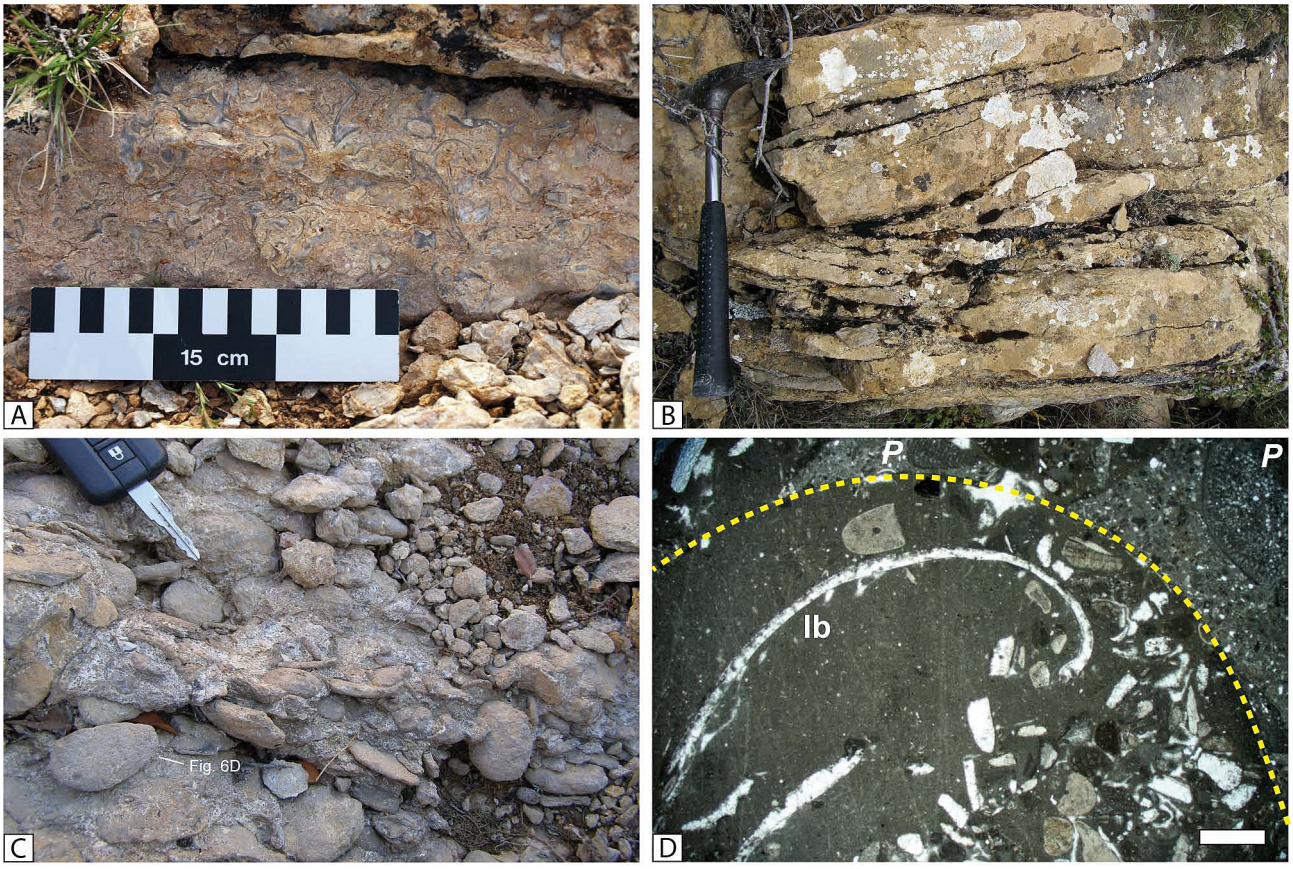

Fig. 6. Sedimentary features of the upper lower Aptian transgressive valley-fill deposits of the Barranco del Portolés. Villarroya de los Pinares Formation, Depositional Sequence B. A) Detail of the early transgressive oyster-bearing limestones. B) Close-up view of bidirectional cross-bedding, interpreted as a result of tides, locally exhibited by the early transgressive oyster-rich grainstones. Hammer = 32 cm. C) Detail of the conglomerate present in the middle part of the early transgressive succession back-filling the incised valley. Visible part of key = 5.4 cm. D) Photomicrograph of a pebble from the conglomerate shown in C. Note that the original texture of the pebble rock was a packstone with *Palorbitolina lenticularis* (*P*) and how the pebble was bored by lithophagid bivalves (lb). The margin of the *Gastrochaenolites* boring is marked with a yellow dashed line. Scale = 1 mm. See Fig. 5 for locations of the images.

Formation in the Barranc del Garrofer quarry is interpreted as a highstand normal regressive unit belonging to Depositional Sequence A (Figs. 2, 7A–B). The highly erosional subaerial unconformity capping this lithostratigraphic unit is also in agreement with a highstand interpretation for these platform carbonates.

The Barranc del Garrofer quarry is the only outcrop in the northeastern Orpesa Sub-basin where the Villarroya de los Pinares Formation and thus, the surface of subaerial exposure and erosion surmounting this unit, have been recognised (Fig. 1B, D). Therefore, the extension within this depocentre of this incised subaerial unconformity, which formed during a late early Aptian forced regression of Depositional Sequence A, is unknown. However, the flat-ramp erosional profile and the incision depth of c. 10 m exhibited by the surface are in accordance with strath terraces carved into bedrock of a valley-side slope (Fig. 7A–B). Dimensions of incised valleys encompass depths ranging from just a few to several tens of metres, along with widths spanning from 1 to 10 km (see, for example, Horozal et al., 2021 and references therein).

During the subsequent transgression of terminal early–earliest late Aptian age, the incision was infilled with marly deposits and high-energy grainstone textures dominated by large-sized discoidal orbitolinids (Fig. 7D). These transgressive deposits, which belong to Depositional Sequence B, onlap the ramps and overlie the flat segments of the terraces (Fig. 7A–B). Above this succession of marls and grainstone limestones with orbitolinids, massive thicker beds with floatstone to rudstone textures containing rudists and *Chondrodonta* are interpreted as proximal platform top facies and therefore, as regressive deposits (Fig. 7A–B).

4.1.3. El Regajo

4.1.3.1. Sedimentary and palaeontological description. Above the ammonite-bearing marls, marly limestones and packstone limestones with *Palorbitolina lenticularis*, *Praeorbitolina* and *Choffatella decipiens* of the Forcall Formation, a reduced in extent (c. 100 m in length) and thickness (c. 6 m) carbonate platform succession crops out in two dimensions (Fig. 8A–B) to the West of Miravete de la Sierra (Fig. 1C). The succession belongs to the Villarroya de los Pinares Formation and is constituted by four limestone beds (1–4 in Fig. 8B) with an approximate thickness about 1.5 m each stacked in a backstepping fashion (Fig. 8A–B).

The first layer exhibits a rudstone texture dominated by oysters (Fig. 8C). This oyster-bearing limestone bed originates in El Regajo and progressively evolves southwards for 2.3 km to La Serna creek (Fig. 1C), to a tidal-influenced thicker unit (up to c. 21 m) composed of various beds (see Bover-Arnal et al., 2015). Other non-skeletal and skeletal components identified in this first bed include peloids, intraclasts, *Palorbitolina lenticularis* (Fig. 8C), miliolids, encrusting foraminifera, other benthic foraminifera, serpulids, bryozoans, and fragments of echinoids, other molluscs and crustaceans. The second bed (Fig. 8B) exhibits a floatstone–rudstone texture rich in oysters and corals. Peloids, benthic foraminifera, encrusting foraminifera and fragments of other bivalves, gastropods, echinoids, serpulids and dasycladaceans are also common components found in this latter layer. The third limestone bed has a floatstone texture dominated by colonies of scleractinian corals and other components such as encrusting and other benthic foraminifera, fragments of molluscs and echinoids, and peloids. The last stage of

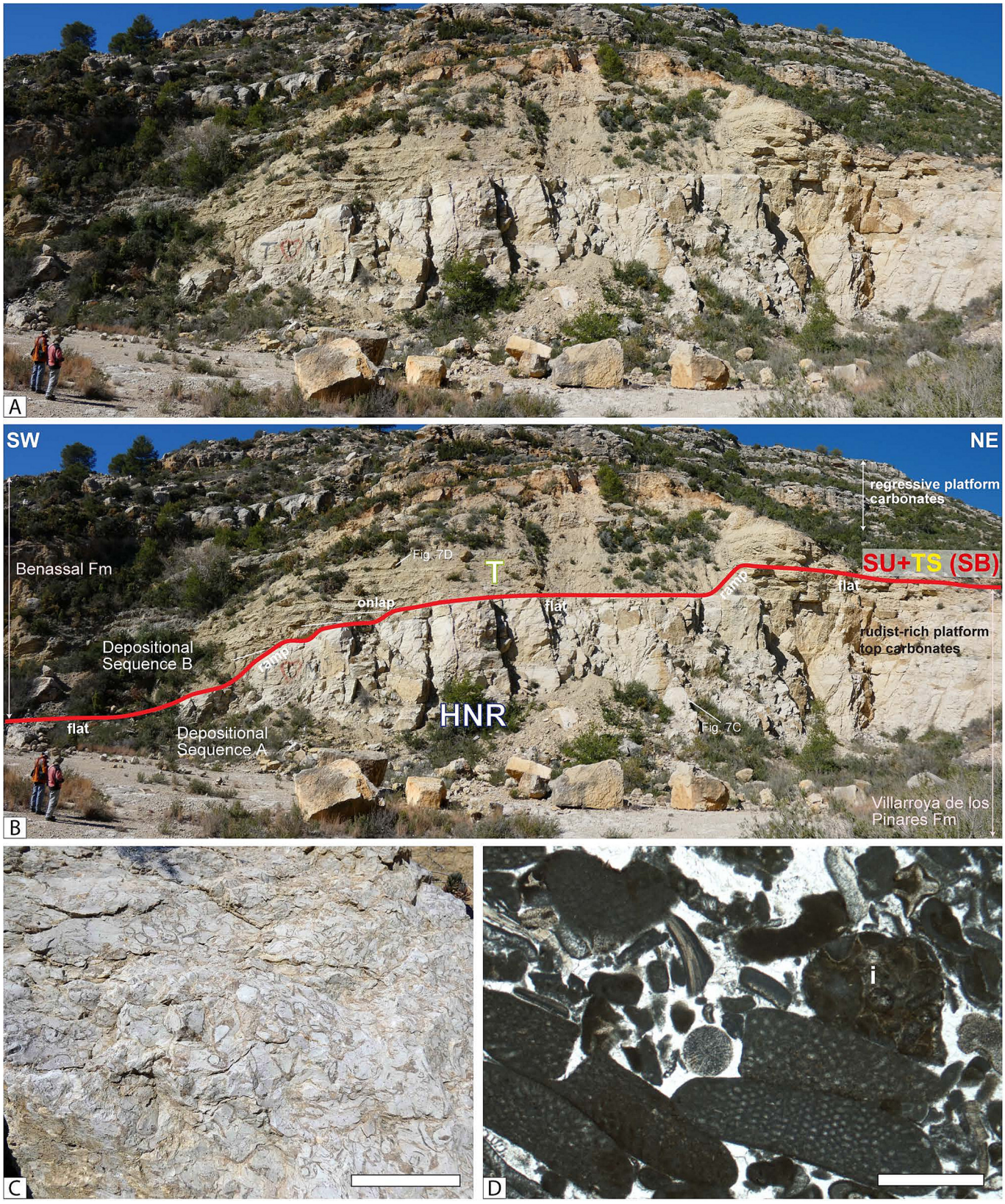

Fig. 7. Barranc del Garrofer quarry. A) Panoramic view. B) Interpretation of A including the lithostratigraphic units, the sequence-stratigraphic framework, and the location of C–D. Note the incised subaerial unconformity (SU) with flats and ramps cutting downwards the highstand platform carbonates of the Villarroya de los Pinares Formation and how the transgressive marls and limestones of the lower part of the Benassal Formation back-filled the palaeovalley created. Width of image = c. 80 m. See Fig. 4 for key. C) Detail of a rudist biostrome belonging to the highstand platform top carbonates of the Villarroya de los Pinares Formation (Depositional Sequence A). Scale bar = 8 cm. See B for location of the photographed outcrop. D) Photomicrograph of a grainstone texture dominated by large-sized discoidal orbitolinids located at the transgressive, lower part of the Benassal Formation (Depositional Sequence B). Note the presence of an intraclast (i). Scale bar = 1 mm.

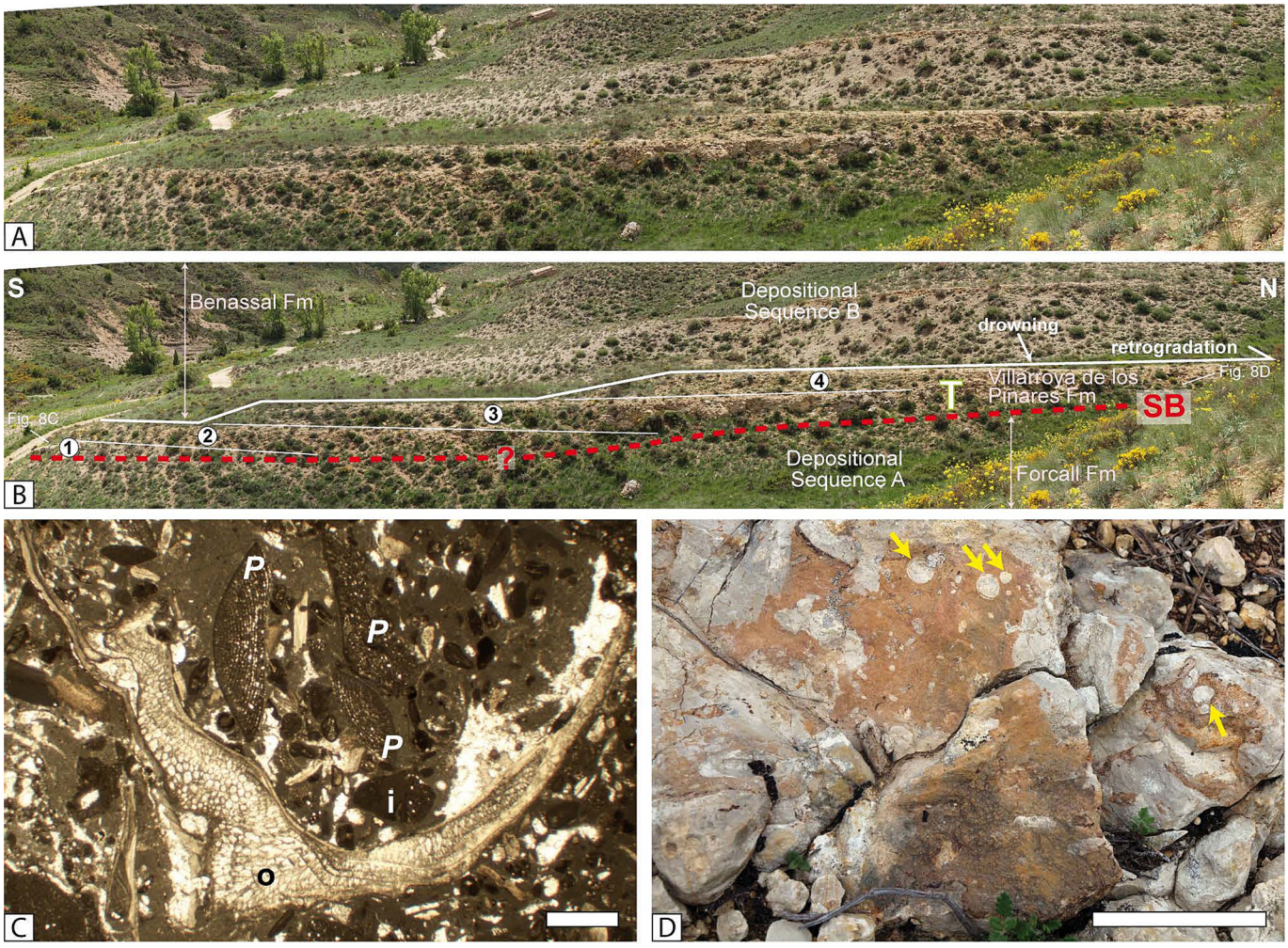

Fig. 8. El Regajo. A) Panoramic view of El Regajo retrograding carbonate platform. B) Interpretation of A including the lithostratigraphic units, the sequence stratigraphic framework, and the location of C–D. Numbers 1–4 correspond to stratigraphic beds described in the text. Width of image = c. 100 m. See Fig. 4 for key. C) Photomicrograph of a rudstone texture containing oysters (o), intraclasts (i) and *Palorbitolina lenticularis* (P) Scale bar = 1 mm. See B for location of the microphotographed sample. Scale bar = 1 mm. D) Close-up view of a coral colony exhibiting *Gastrochaenolites* (yellow arrows). Scale bar = 5 cm.

carbonate platform development generated a floatstone bed dominated by colonial corals (Fig. 8D) that also includes peloids, oysters, gastropods, other molluscs, miliolids, orbitolinids, encrusting foraminifera, other benthic foraminifera, serpulids, echinoderms and bryozoans.

Above this fourth carbonate platform bed, the marls of the lowermost part of the Benassal Formation occur (Fig. 8A–B). This marl unit is characterised by the presence of large gastropods, which were identified as *Trochonerita gigas* by Bover-Arnal et al. (2010) and are characteristic of the lower part of the Benassal Formation in the Galve Sub-basin. Upwards in the succession, the marls of the basal part of the Benassal Formation are interbedded with limestones and marly limestones with *Mesorbitolina*.

4.1.3.2. Depositional and sequence-stratigraphic interpretation. The small carbonate platform of El Regajo belonging to the Villarroya de los Pinares Formation (Fig. 8) is located approximately 1 km to the south of the platform-to-basin transition area of Las Mingachas (Fig. 1C) (see Bover-Arnal et al., 2009, 2022). In this regard, the El Regajo platform is located basinwards, disconnected from the platform carbonates of Las Mingachas. The four limestone beds described in El Regajo exhibit an original horizontal layering and contain abundant colonial corals and oysters, and thus are interpreted to represent a platform top setting. Noteworthy is that rudist shells were not identified in the isolated platform of El Regajo, or at least are not common. This contrasts with the situation at Las Mingachas, where rudists are dominant in the highstand, lowstand and transgressive platform top carbonates of the Villarroya de los Pinares Formation (see Bover-Arnal et al., 2009, 2022).

The platform carbonates of El Regajo are stacked in a retrograding pattern, indicating that they were deposited during a transgressive context (Fig. 8B). The underlying basinal marls and limestones of the Forcall Formation contain *Palorbitolina lenticularis* and *Praeorbitolina* that indicate a late early Aptian age (Cherchi and Schroeder, 2013). The first limestone bed of El Regajo carbonate platform (Fig. 8B) also includes *Palorbitolina lenticularis* (Fig. 8C). Accordingly, the age of El Regajo isolated platform is latest early Aptian.

The oyster-bearing basal deposit of the El Regajo platform (Fig. 8B–C) is continuous to La Serna creek (Fig. 1C) where it exhibits tidal bundles and onlaps or overlies a composite sequence boundary (a transgressive surface superposed onto a subaerial unconformity) incised in highstand platform carbonates and marls of Depositional Sequence A (Bover-Arnal et al., 2015). However, clear sedimentary records of subaerial exposure at the top of the marls of the Forcall Formation were not identified in El Regajo.

The backstepping carbonate platform of El Regajo is onlapping an irregular palaeotopography (Fig. 8A–B). This irregular surface, which corresponds to a sequence boundary (Fig. 8B), bounds basinal marls (Forcall Formation) of Depositional Sequence A from transgressive carbonates (Villarroya de los Pinares Formation) of Depositional

Sequence B. To the North, in the nearby outcrop of Las Mingachas (Fig. 1C) and towards the basin, the sequence boundary corresponds to a correlative conformity (Bover-Arnal et al., 2009, 2022). The irregular surface below the platform carbonates of El Regajo (Fig. 8B) might correspond to the basinwards continuation of the correlative conformity interpreted in Las Mingachas (Fig. 1C) (Bover-Arnal et al., 2009, 2022). This correlative conformity would have been then superposed by a transgressive surface at the onset of transgression during Depositional Sequence B. Erosion during base-level fall (Depositional Sequence A) or transgression (Depositional sequence B) could also account for the irregular palaeorelief at the top of the marls of the Forcall Formation. In this regard, the sequence boundary would respectively correspond to a regressive surface of marine erosion or to a transgressive ravinement surface (see Catuneanu et al., 2009).

The limestone beds stacked in a retrograding pattern found in El Regajo indicate that carbonate production was outpaced by the rate of relative sea-level rise, and thus the small, isolated platform backstepped prior to drowning (Fig. 8A–B). This episode of platform development in El Regajo might have been coeval to the lowstand and/or early transgressive stages of Depositional Sequence B recorded in Las Mingachas (see Bover-Arnal et al., 2009, 2022). If the retrograding stacking pattern recorded in El Regajo was contemporaneous with the development of a prograding and aggrading lowstand platform in Las Mingachas, it would suggest that the carbonate factory established in Las Mingachas was more robust and efficient than the one that flourished in El Regajo. This possibility is consistent with the field observations (compare Fig. 8A–B in this paper with Fig. 6B–C in Bover-Arnal et al., 2022). The occurrence of distinct stacking patterns in coeval and close by or adjacent carbonate platforms has been documented in more recent carbonate platforms, such as in the Bahamas (e.g., Eberli and Ginsburg, 1987). In the Bahamas carbonate platform, during the mid-Oligocene to mid-Miocene, the Andros Bank was prograding in the Andros Straits, whilst the Bimini Bank was aggrading in the Straits of Florida. In contrast, from the mid-Miocene to the present day, the Great Bahama Bank has been aggrading in the Straits of Andros and prograding in the Straits of Florida (Eberli and Ginsburg, 1987).

4.2. Early late Aptian examples of major relative sea-level change

4.2.1. Las Cubetas

4.2.1.1. Sedimentary and palaeontological description. The sedimentary evolution of the lower part of the Benassal Formation in Las Cubetas commences with a 10 m-thick marl interval (Fig. 9A–C). Above, a 9 m-thick aggrading succession of bioturbated bluish limestones rich in fragments of *Permocalculus* occurs (Figs. 9A–C, 10A–B). The limestones mainly exhibit packstone textures and include peloids, miliolids, other benthic foraminifera and fragments of molluscs and echinoids (Fig. 10A). The uppermost bed of this *Permocalculus*-rich unit (metres 1.5 to 3) (Fig. 10A–B) contains scarce ooids and other coated grains, lituolids, textularids, sections of serpulids and rare fragments of gastropods, oysters, brachiopods, bryozoans and peysonneliaceans.

The surface topping the latter limestone bed is uneven and marks a change in lithofacies. From metres 3 to 4, a yellowish grainstone (Figs. 9B–C, 10A), which is dominated by *Permocalculus* debris in its lower part and by ooids in its upper part (Fig. 10C), occurs. Peloids, rare lituolids and miliolids, other benthic foraminifera and fragments of molluscs, serpulids and echinoids are also present. The top of this grainstone layer corresponds to a hardground surface (Fig. 10A) displaying ferruginous stains. Overlying this hardground, there is a 1.2 m-thick yellowish grainstone unit subdivided by faint bedding planes (Figs. 9B–C, 10A), which is topped by a well-developed hardground with iron oxides and abundant encrusting oysters (Fig. 9D). The grainstone package contains abundant *Permocalculus* debris, as well as intraclasts, scarce ooids, textularids, other benthic foraminifera, serpulids, and fragments of nerineid gastropods, oysters, other molluscs, coral and echinoids. The succession continues with marls, which also belong to the Benassal Formation, and exhibit an interval with calcareous nodules in their lower part (Fig. 10A).

4.2.1.2. Depositional and sequence-stratigraphic interpretation. Above the platform top carbonates with rudists of the Villarroya de los Pinares Formation (Fig. 9A), the distal platform marls of the base of the Benassal Formation are interpreted as transgressive deposits of Depositional Sequence B (Fig. 9). The maximum flooding surface of the sequence was placed at the top of the marl interval and below the first downlap surface of the overlying *Permocalculus*-rich bioturbated limestone unit. The *Permocalculus*-bearing succession mainly exhibits packstone textures, shows an aggradding pattern and terminates with an irregular surface with hollows. This surface is overlain by a yellowish grainstone succession dominated by ooids (Fig. 10C) and *Permocalculus* debris (Fig. 10A). The facies evolution described shares similarities to that observed in the Loma de Camarillas section (see Bover-Arnal et al., 2022), which is located in the western limb of the Miravete anticline (Fig. 1C). In addition, the uneven surface identified in Las Cubetas is located at the same stratigraphic position as the major sequence boundary with palaeokarst of early late Aptian age identified in the Loma de Camarillas site (see Bover-Arnal et al., 2022). Accordingly, the aggrading packstones with *Permocalculus* are interpreted to have been deposited during a highstand normal regressive stage (Depositional Sequence B). The irregular surface topping these highstand platform carbonates is interpreted as a subaerial unconformity recording a major relative sea-level fall (Figs. 9B–C, 10A).

During the subsequent marine flooding, a transgressive surface developed onto the subaerial unconformity giving rise to a rockground (composite sequence boundary). It was covered by higher-energy transgressive grainstones with ooids and *Permocalculus* debris belonging to Depositional Sequence C (Figs. 9B–C, 10A). In the course of the early phase of the transgression, the carbonate factory sourcing these higher-energy deposits drowned. Drowning is marked by a conspicuous hardground surface with encrusting oysters (Fig. 9D) that was buried by distal platform marls (Fig. 9B-C).

In this example, the absence of geometries presents a certain level of complexity in comprehending the sequence-stratigraphic interpretation. Nonetheless, it would be prudent to underscore two pertinent aspects: Firstly, the incorporation of regional criteria derived from other outcrops exhibiting well-defined geometries (see the late Aptian case studies in Bover-Arnal et al., 2022) that corroborate the proposed interpretation. This regional perspective contributes to the broader understanding of the stratigraphic context. Secondly, the significance of this case study as an illustrative example for interpreting sequence boundaries and deciphering the sequence-stratigraphic arrangement in vertical successions of platform carbonates.

4.2.2. Estrecho de la Calzada Vieja

4.2.2.1. Sedimentary and palaeontological description. The stratigraphic succession logged in the Estrecho de la Calzada Vieja covers the uppermost part of the first limestone horizon of the Benassal Formation (Fig. 11A–D). This horizon consists of aggrading platform carbonates with a thickness of about 18 m. It overlies a c. 25 m-thick marl interval (Fig. 11A–B) containing gastropods and levels with scleractinian corals that distinguishes the lowermost part of the Benassal Formation (Fig. 2). The sedimentary succession measured and sampled (Fig. 11C–D) commences with a bioturbated greyish 1.5 m-thick grainstone with abundant fragments of *Permocalculus* and tests of *Mesorbitolina* (Fig. 12A–B). Other skeletal components include lituolids, undetermined benthic foraminifera, and fragments of molluscs, echinoids and bryozoans, whereas the non-skeletal components correspond to peloids, ooids, other coated grains and scarce intraclasts (Fig. 12A).

The top of the grainstone bed is slightly erosional (Figs. 11E, 12A), and locally, exhibits palaeokarst features. It is succeeded by a yellowish

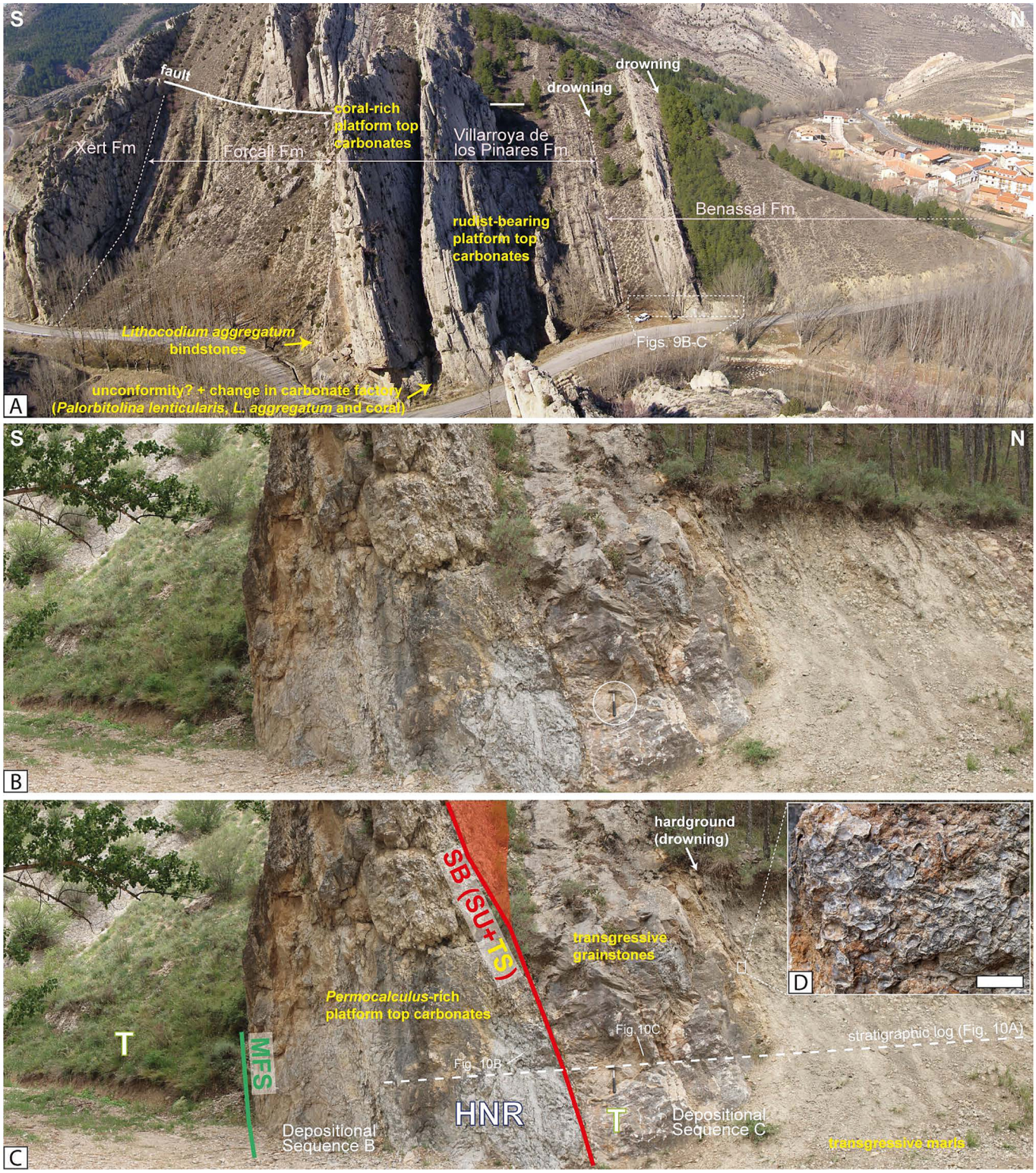

Fig. 9. Las Cubetas. A) Interpreted panoramic photomosaic of Las Cubetas section near Aliaga including the lithostratigraphic units, key facies and stratigraphic surfaces, and the situation of B–C. Width of image = c. 350 m. B) Outcrop view showing the lower upper Aptian composite sequence boundary (SU + TS) between depositional sequences B and C within the lower part of the Benassal Formation. Hammer = 32 cm. C) Interpretation of B including the sequence-stratigraphic analysis, the main facies, the location of Fig. 10B–C, and the stratigraphic log shown in Fig. 10A. Hammer = 32 cm. See Fig. 4 for key. D) Detail of a hardground surface with encrusting oysters and iron oxides capping the transgressive grainstones with ooids and *Permocalculus* debris of Depositional Sequence C. This hardground marks the drowning of the platform carbonates of the lower part of the Benassal Formation.

20 cm-thick grainstone dominated by ooids (Fig. 12C), that also includes intraclasts, peloids, scarce *Permocalculus* debris, *Mesorbitolina*, lituolids, miliolids, other benthic foraminifera, as well as fragments of echinoids, bryozoans, oysters, other bivalves and gastropods (Fig. 12A). The succession continues with a yellowish to orange c. 2 m-thick cross-bedded (Fig. 11F) grainstone unit rich in ooids, with scarce to common peloids, intraclasts, serpulids, *Mesorbitolina*, lituolids, miliolids, other benthic foraminifera, and fragments of *Permocalculus*, bryozoans, echinoids, crinoids, gastropods, oysters and other bivalves (Fig. 12A). Above, there is a marl bed up to 10 m-thick.

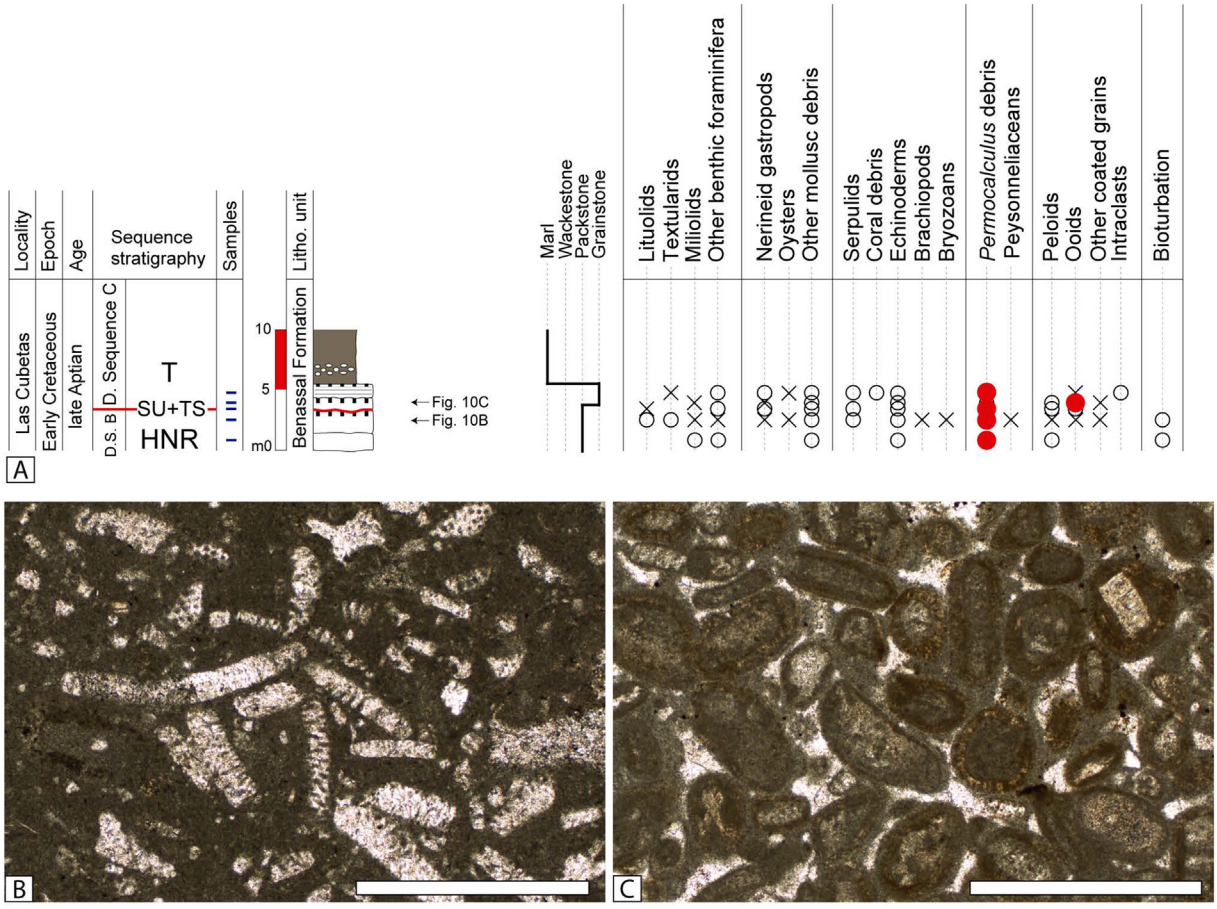

Fig. 10. Las Cubetas. A) Sedimentary log of the lower upper Aptian strata underlying and overlying the composite sequence boundary between depositional sequences B and C in Las Cubetas road section. The stratigraphic section displays the sequence-stratigraphy analysis, the stratigraphic position of the samples collected, the lithostratigraphic units, the lithology, the bedding, the textures, the sedimentary features, the location of photographs in B–C, and the stratigraphic position of the skeletal and non-skeletal components identified. See Fig. 9C for location of the section. See Fig. 5 for key. B) Packstone texture dominated by fragments of *Permocalculus* belonging to the highstand normal regressive deposits of the lower part of the Benassal Formation (early late Aptian). Depositional Sequence C. Scale = 1 mm. See Figs. 9C and 10A for location. C) Photomicrograph of an ooid grainstone of the basal transgressive deposits of Depositional Sequence C (early late Aptian). Benassal Formation. Scale = 1 mm. See Figs. 9C and 10A for location.

4.2.2.2. Depositional and sequence-stratigraphic interpretation. The lower part of the Benassal Formation in the Estrecho de la Calzada Vieja is characterised by transgressive distal platform marls and aggrading highstand normal regressive packstones and grainstones with *Permocalculus* debris of Depositional Sequence B (Figs. 11A–B, 12A–B). The maximum flooding surface is interpreted to correspond to the first downlap surface of the lower upper Aptian *Permocalculus*-bearing limestones above the deeper marls. A major relative sea-level fall, which occurred during the early late Aptian, exposed subaerially and eroded the top of the highstand *Permocalculus*-rich deposits (Fig. 11).

With the subsequent transgression of Depositional Sequence C, a transgressive surface was superposed onto the subaerial unconformity giving rise to a composite sequence boundary, which corresponds to a rockground (Figs. 11, 12A). During the earliest stage of the transgression, shallow high-energy ooidal limestones were deposited (Fig. 12C). These cross-bedded carbonates were drowned during early stages of transgression and were buried by transgressive distal platform marls (Figs. 11C–F, 12A). The transgressive succession of Depositional Sequence C described is also part of the Benassal Formation.

5. Discussion

5.1. The Maestrat Basin record of Aptian relative sea-level change

In addition to the five outcrops investigated in the present paper, ten further previously published examples showing evidence of major Aptian relative sea-level fluctuations from other geological sites within the Maestrat Basin (Fig. 1B–C) will be considered in this section's discussion. The previously studied outcrops include the Mola de la Garumba, Mola d'en Camaràs, and Ulldecona in the Morella Sub-basin (Fig. 1B) (Bover-Arnal et al., 2014, 2022; Bover-Arnal and Salas, 2019), Las Mingachas, La Serna, Loma de Camarillas, Barranco de la Canal, Campillo Bajo, and Camino de Camarillas in the Galve Sub-basin (Fig. 1B) (Bover-Arnal et al., 2009, 2015, 2022), and the Orpesa Range in the Orpesa Sub-basin (Fig. 1B) (Martín-Martín et al., 2013; Yao et al., 2020). The features of the different sedimentary records of major falls and rises in relative sea level characterised in Aptian rocks from the Maestrat Basin, including the previously published case studies, are summarised in Table 1.

The late early Aptian deeply incised truncation surface cutting down the Villarroya de los Pinares and Forcall formations recognised in the Barranco del Portolés in the Galve Sub-basin (Fig. 1C) (Table 1) permits estimating the amplitude of relative sea-level change by measuring the incision depth. This depth is ≥80 m and the incision surface corresponds to the southern side of an incised valley, which is ≥1,8 km in width (Figs. 3, 4). Peropadre Medina (2012) also reported on this palaeovalley and gave a maximum incision depth of 75 m.

In the Orpesa Sub-basin (Fig. 1B) (Table 1), a south-eastern depocentral area of the Maestrat Basin, an erosional surface truncating the platform carbonates of the Villarroya de los Pinares Formation was also identified in the Barranc del Garrofer quarry (Fig. 1D). This erosional incision crops out locally and shows a minimum depth of c. 10 m (Fig. 7A–B).

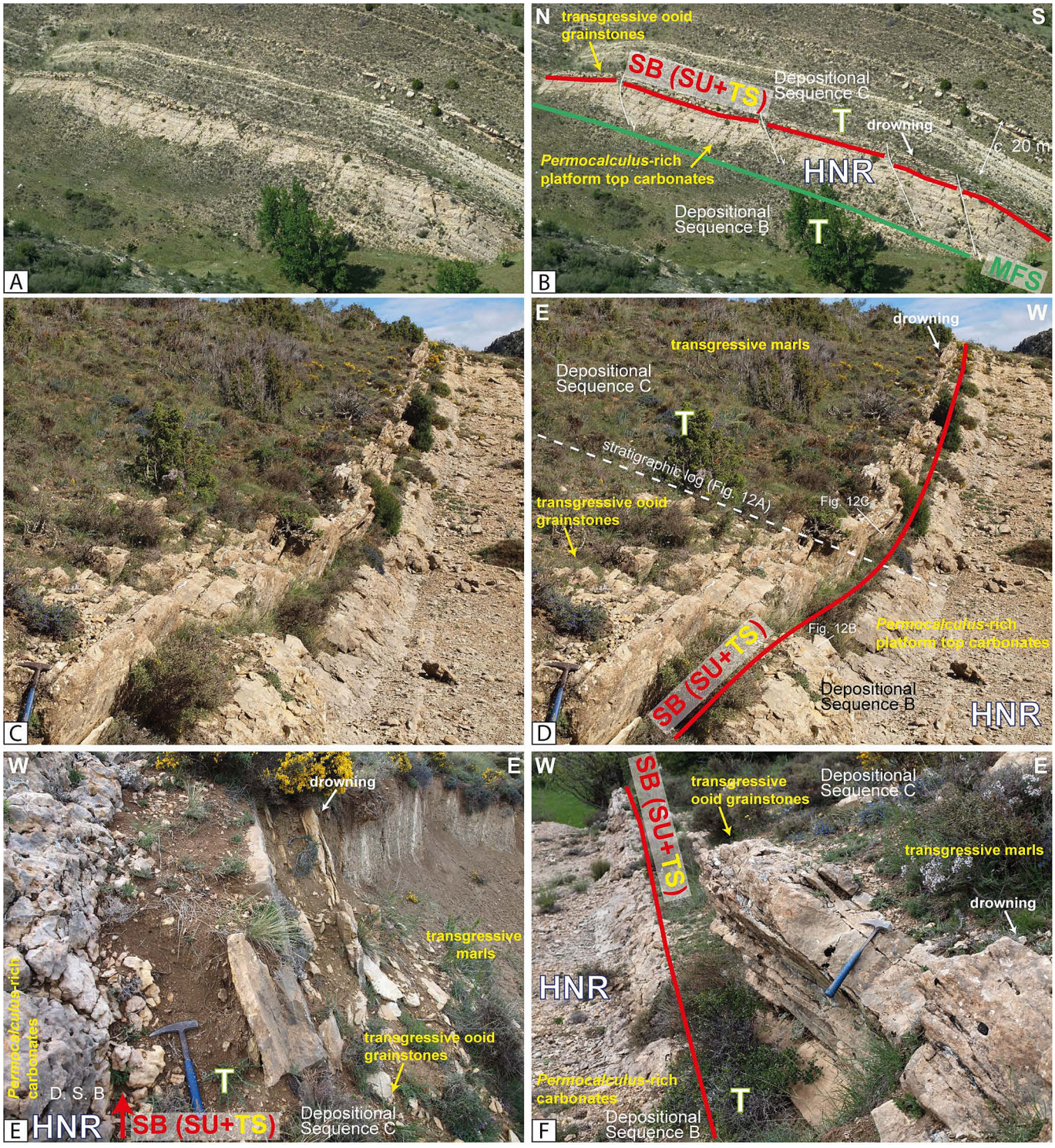

Fig. 11. Estrecho de la Calzada Vieja. A) Panoramic view showing the lower upper Aptian composite sequence boundary (SU + TS) between depositional sequences B and C present in the lower part of the Benassal Formation. B) Interpretation of A including the lithostratigraphic units, key facies and the sequence-stratigraphic interpretation. Note the drowning of the transgressive carbonates and how they were buried by marls of the Benassal Formation. Note also the presence of growth faults. See Figs. 4 and 1C for key and location, respectively. C) Close-up view of the lower upper Aptian composite sequence boundary (SU + TS) between depositional sequences B and C cropping out in the Estrecho de la Calzada Vieja. D) Interpretation of C including the lithostratigraphic units, main facies, the sequence-stratigraphic interpretation, the location of Fig. 12B–C, and the stratigraphic log shown in Fig. 12A. Hammer = 32 cm. See Figs. 4 and 1C for key and location, respectively. E) Detail of the lower upper Aptian subaerially exposed highstand carbonates of Depositional Sequence B overlain by transgressive ooid grainstones and marls of Depositional Sequence C. Note how the transgressive basal grainstones were drowned, and subsequently buried by marls. Benassal Formation. Hammer = 32 cm. See Fig. 4 for key. F) Outcrop view of the lower upper Aptian composite sequence boundary between the highstand platform top carbonates rich in *Permocalculus* of Depositional Sequence B and the higher-energy cross-bedded transgressive ooid grainstones of Depositional Sequence C. Hammer = 32 cm. See Fig. 4 for key.

The deeply incised subaerially exposed platform carbonates of the Villarroya de los Pinares Formation described herein are coeval and analogous to erosional surfaces previously described in outcrops of the Galve Sub-basin (Fig. 1B): La Serna (Bover-Arnal et al., 2015), Barranco de la Canal, Campillo Bajo and Camino de Camarillas (Bover-Arnal et al., 2009, 2010, 2011, 2022). In La Serna (Fig. 1C), an erosional surface cuts

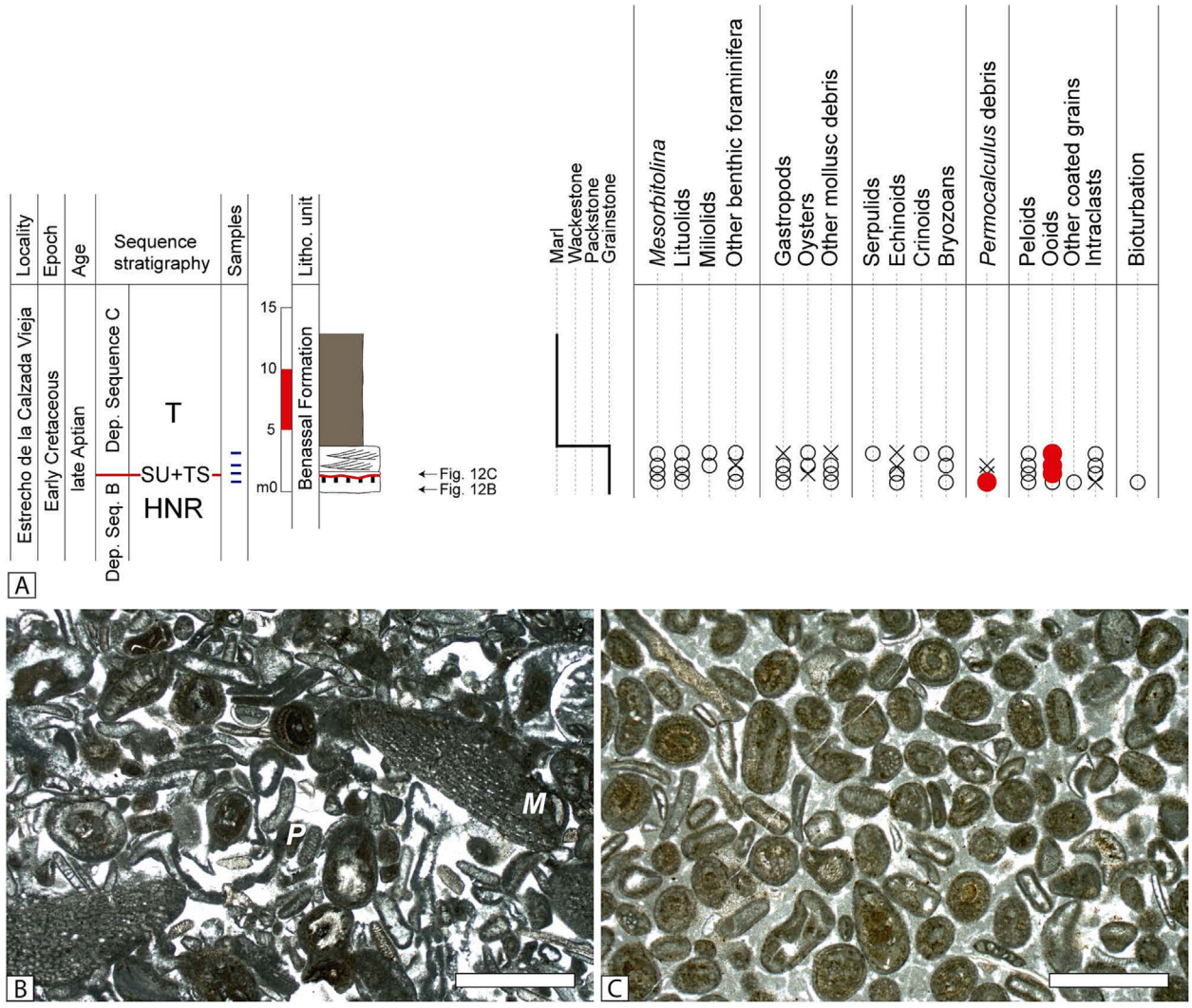

Fig. 12. Estrecho de la Calzada Vieja. A) Sedimentary log of the lower upper Aptian strata underlying and overlying the composite sequence boundary (SU + TS) between depositional sequence B and C in the Estrecho de la Calzada Vieja section. The stratigraphic section displays the sequence-stratigraphy analysis, the stratigraphic position of the samples collected, the lithostratigraphic units and their features (lithology, bedding, textures, sedimentary structures), the location of photographs in B–C, and the stratigraphic position of the skeletal and non-skeletal components identified. See Fig. 11D for location of the section. See Fig. 5 for key. B) Grainstone texture mainly including fragments of *Permocalculus* (*P*) and *Mesorbitolina* (*M*) tests belonging to the highstand normal regressive deposits of the lower part of the Benassal Formation (early late Aptian). Depositional Sequence B. Scale = 1 mm. See Figs. 11D and 12A for location. C) Photomicrograph of an ooid grainstone belonging to the basal transgressive deposits of Depositional Sequence C (early late Aptian). Benassal Formation. Scale = 1 mm. See Figs. 11D and 12A for location.

down an isolated carbonate platform belonging to the Villarroya de los Pinares Formation down to 25 m. This incision erodes the upper part of the Forcall Formation as well. Aggrading platform top carbonates of the Villarroya de los Pinares exposed along the Barranco de la Canal and Campillo Bajo sites (Fig. 1C), exhibit erosional surfaces about 50 and 15 m in depth, respectively.

It is noteworthy that in the Galve Sub-basin, incised erosional profiles associated with the late early Aptian major sea-level drop only occur to the West (hanging wall) of the Miravete fault and have not been recognised so far along the eastern side footwall (Fig. 1C), where the thickness of the Barremian–Aptian stratigraphic units and facies indicate lower accommodation and shallower depositional settings than those of the western side (e.g., Simón et al., 1998; Bover-Arnal et al., 2010). Similarly, upper lower Aptian tidally-influenced deposits back-filling topographic lows have neither been observed to the East of the Miravete fault.

Nevertheless, on the eastern side footwall (Fig. 1C), a succession of coral-rich platform top limestones corresponding to the lower part of the Villarroya de los Pinares Formation is interrupted by a slightly irregular surface (Fig. 9A) exhibiting rounded dissolution pits and iron oxide-rich crusts. This conspicuous surface can be laterally followed from the Estrecho de la Calzada Vieja to Las Cubetas (Fig. 1C) (Table 1), where it is overlain by rock-forming *P. lenticularis* grainstones, *Lithocodium aggregatum*-bearing deposits and marls with scleractinians in life position (Fig. 9A). Above this succession recording a change in the carbonate factory, platform limestones with rudists occur. This surface (Fig. 9A) recognised in the eastern limb of the Miravete anticline (Fig. 1C) is probably correlatable with the upper lower Aptian subaerial unconformity documented by Bover-Arnal et al. (2015, 2022) in the Barranco de la Canal, Campillo Bajo, Camino de Camarillas and La Serna (Fig. 1C), as well as in the Barranco del Portolés outcrop described herein (Figs. 3, 4). Vennin and Aurell (2001) and Embry et al. (2010) already placed a major sequence boundary at this surface (SB2 in Vennin and Aurell, 2001 and SBII-I in Embry et al., 2010) and documented signs of emersion such as the presence of meteoric vadose cements.

The lack of upper lower Aptian incised valleys on the eastern side of the Miravete fault foot wall (Fig. 1C) is interpreted as due to two causes. Firstly, stream or river incisions on bedrock develop as local features, as observed in other Aptian (e.g., Raven et al., 2010), Messinian (e.g., Pellen et al., 2019) or Quaternary (e.g., Wang et al., 2019) examples. That is,

Table 1
Summary of the results for the different outcrops with a record of Aptian major relative sea-level fluctuations investigated and discussed from the Maestrat Basin.

Age	Outcrop	Sub-basin	Lithostratigraphic unit showing a record of sea-level fall	Lithostratigraphic unit showing a record of succeeding base-level rise	Sedimentary features representing sea-level fall	Incised-valley development	Depth of incised valley (m)	Palaeokarst development
Early late Aptian	Estrecho de la Calzada Vieja	Galve	Benassal	Benassal	Subaerial unconformity	No	N/A	Yes
	Las Cubetas	Galve	Benassal	Benassal	Subaerial unconformity	No	N/A	Not recognised
	Loma de Camarillas[e]	Galve	Benassal	Benassal	Subaerial erosional truncation	No	N/A	Yes
	Orpesa Range[d]	Orpesa	Benassal	Benassal	Maximum regressive surface	N/A	N/A	N/A
	Ulldecona[b]	Morella	Benassal	Benassal	Maximum regressive surface	N/A	N/A	N/A
	Mola d'en Camaràs[a,e]	Morella	Benassal	Benassal	Subaerial erosional truncation	Yes	≥ 115	Yes
Late early Aptian	Barranco del Portolés	Galve	Villarroya de los Pinares	Villarroya de los Pinares and Benassal	Subaerial erosional truncation	Yes	≥ 80	Not recognised
	El Regajo	Galve	Villarroya de los Pinares	Villarroya de los Pinares and Benassal	Correlative conformity?	N/A	N/A	Not recognised
	Barranc del Garrofer quarry	La Salzedella	Villarroya de los Pinares	Benassal	Subaerial erosional truncation	Yes	≥ 10	Unknown
	Barranco de la Canal[e,f]	Galve	Villarroya de los Pinares	Villarroya de los Pinares and Benassal	Subaerial erosional truncation	Yes	≥ 50	Yes
	Campillo Bajo[e]	Galve	Villarroya de los Pinares	Villarroya de los Pinares and Benassal	Subaerial erosional truncation	Yes	≥ 15	Yes
	Camino de Camarillas[e]	Galve	Villarroya de los Pinares	Villarroya de los Pinares and Benassal	Subaerial erosional truncation	More likely	Unknown	Yes
	Las Mingachas[e,f]	Galve	Villarroya de los Pinares	Villarroya de los Pinares and Benassal	Forced regressive wedge	N/A	N/A	N/A
	Orpesa Range[d]	Orpesa	Villarroya de los Pinares	Benassal	Maximum regressive surface	N/A	N/A	N/A
	La Serna[c]	Galve	Villarroya de los Pinares	Villarroya de los Pinares and Benassal	Subaerial erosional truncation	Yes	21	Yes
	Ulldecona[b]	Morella	Villarroya de los Pinares	Benassal	Maximum regressive surface	N/A	N/A	N/A
	Mola de la Garumba[a]	Morella	Villarroya de los Pinares	Villarroya de los Pinares and Benassal	Forced regressive wedge	N/A	N/A	N/A

N/A = not applicable.
[a] Bover-Arnal et al. (2014).
[b] Bover-Arnal and Salas (2019).
[c] Bover-Arnal et al. (2015).
[d] Martín-Martín et al. (2013) and Yao et al. (2020).
[e] Bover-Arnal et al. (2022).
[f] Bover-Arnal et al. (2009).

limestone bedrocks are not always incised during relative sea-level fall and subaerial exposure. The same holds true for karstification. For example, sea-level drops and subaerial exposure episodes recorded during the Last Interglacial in The Bahamas and Florida platforms were manifested as wave-cut benches (e.g., Skrivanek et al., 2018), by the sedimentation of beach and eolian deposits (e.g., Dyer et al., 2021), or as terra rossa palaeosols or calcretes (e.g., Dutton et al., 2022). These sedimentary horizons of subaerial exposure can be later eroded during the subsequent transgression. Secondly, streams and drainage systems are mainly encased on topographic lows and therefore, develop on fault hanging walls (e.g., Goldsworthy and Jackson, 2000).

Other sedimentary features representing relative sea-level fall recorded in the Maestrat Basin for the late early Aptian are forced regressive wedges (Table 1). Forced regressive deposits have been recognised in Las Mingachas (Galve Sub-basin; Bover-Arnal et al., 2009, 2022) and in La Mola de la Garumba (Morella Sub-basin; Bover-Arnal et al., 2014). These basin floor components correspond to cross-bedded grainstones, which include intraclasts and overlie basinal marly deposits. The forced regressive wedges are overlain and downlapped by lowstand platforms that recorded the subsequent rise in base level.

The newly discovered retrograding isolated carbonate platform of El Regajo (Fig. 8) located basinwards (southwards) of the platform-to-basin transition area of Las Mingachas (Fig. 1C) (Bover-Arnal et al., 2009, 2022) provides further evidence of a major relative sea-level fall and rise during the late early Aptian. The El Regajo coral-dominated platform is underlain and overlain by distal, basinal marly deposits rich in *Palorbitolina lenticularis* and ammonoids. The area between El Regajo and Las Mingachas is not significantly tectonised (Fig. 1C). The El Regajo platform crops out at a height of around 1270 m and thus, is found topographically below the highstand and lowstand platforms of Las Mingachas (Fig. 1C) (Bover-Arnal et al., 2009, 2022) that are respectively located at heights of about 1350 m and 1300 m.

A subaerial unconformity resulting from major relative sea-level fall during the early late Aptian is well exposed in Las Cubetas (Figs. 1C, 9–10) and the Barranco de la Calzada Vieja (Figs. 1C, 11–12), along the eastern limb of the Miravete anticline (Fig. 1C). This surface of subaerial exposure (Figs. 9–12), which was overlooked by previous studies carried out on these two sites (Vennin and Aurell, 2001; Bover-Arnal et al., 2010; Embry et al., 2010), is herein characterised to the East of the Miravete fault (foot wall) for the first time (Fig. 1C) together with a facies analysis of the underlying and overlying rocks (Figs. 9–12). This lower upper Aptian emersion surface contained within the lower part of the Benassal Formation bounds depositional sequences B and C (Fig. 2) and is correlatable to the slightly incised subaerial unconformity reported by Bover-Arnal et al. (2022) on the Loma de Camarillas site, to the West of the Miravete fault (hanging wall), within the Galve Sub-basin (Fig. 1C). On both sides of the Miravete fault, this subaerial unconformity locally shows palaeokarst features (Table 1) and is overlain by cross-bedded grainstone textures. These higher-energy transgressive deposits are rich in ooids (Figs. 10B, 12B)

on the eastern side of the Miravete fault, whereas on the western side they contain abundant fragments of crinoids (Bover-Arnal et al., 2022).

At a basin scale, the lower upper Aptian subaerial unconformity reported from the Galve Sub-basin is equivalent to that found in La Mola d'en Camaràs, in the Morella Sub-basin (Fig. 1B) (Table 1). In La Mola d'en Camaràs, this surface of subaerial exposure is deeply incised and exhibits a minimum depth of 115 m and a width of >2 km (Bover-Arnal et al., 2014, 2022), and thus it corresponds to an incised valley. The measured depth of this palaeovalley is indicative of the amplitude of relative sea-level fall and rise recorded during the early late Aptian.

Major relative sea-level falls and rises of late early and early late Aptian age have also been documented from other areas of the Maestrat Basin (Table 1). In the Orpesa Range (Orpesa Sub-basin) (Fig. 1B), Martín-Martín et al. (2013) and Yao et al. (2020) distinguished two major sequence boundaries corresponding to maximum regressive surfaces of late early and of early late Aptian age capping regressive platform carbonates of the Villarroya de los Pinares Formation and the lower part of the Benassal Formation, respectively. Similarly, in Ulldecona (western Morella Sub-basin) (Fig. 1B), Bover-Arnal and Salas (2019) also discussed an upper lower Aptian maximum regressive surface marking the top of the Villarroya de los Pinares Formation, as well as the regressive character for the lower upper Aptian platform carbonates with rudists of the Benassal Formation. Therefore, the late early and early late Aptian relative sea-level changes studied, as well as the related incised valleys documented herein and in Bover-Arnal et al. (2022), had at least a regional, basin-wide significance.

5.2. Comparable Aptian records of relative sea-level change from other basins worldwide

The major late early and early late Aptian relative sea-level changes interpreted in the Maestrat Basin had amplitudes of between 50 and 80 m and about 115 m, respectively (Table 1). The late early Aptian fall and rise of relative sea level had a duration of <0.9 Myr, whereas the duration of the late early Aptian relative sea-level event was <3 Myr (see Bover-Arnal et al., 2022). Amplitudes of relative sea-level change of tens of metres occurring in <1 Myr would be in agreement with eustatic, perhaps glacio-eustatic, controls (Immenhauser, 2005; Miller et al., 2005; Ray et al., 2019).

The Maestrat Basin resulted from rifting (Salas et al., 2001, 2010), and thus tectonics played a part in controlling accommodation during the Aptian. Differential subsidence within the basin during this stage is evidenced by the recorded thicknesses of the sedimentary successions, which range from few metres (e.g., Salas, 1987) to over 1.3 km (e.g., Yao et al., 2020). Nevertheless, the late early–early late Aptian time interval studied corresponded to a period of slow synrift subsidence in the western Maestrat Basin (Bover-Arnal et al., 2010).

Moreover, the strata filling the upper lower Aptian incised valley documented in the Barranco del Portolés (Fig. 4) show a similar dip and dip direction as the incised highstand strata (Fig. 3). A scenario of rock layers experiencing an uplift of c. 80 m without folding or tilting, followed by subaerial exposure, incision, and subsequent subsidence of the same magnitude without folding or tilting whilst marine sedimentation resumes, all within a time span of less than 0.9 Myr, appears improbable. As discussed in Bover-Arnal et al. (2022) for other Aptian incised valleys recorded in the Maestrat Basin, this lack of stratal angularity between the truncated succession below and the back-filling deposits above is interpreted as absence of tilting during relative sea-level fall and subsequent rise, and thus as resulting mainly from eustasy. Accordingly, coeval and similar major changes in accommodation should be observable in other basins of the Tethys and beyond.

Possible coeval major sea-level fluctuations have been recognised in other Aptian successions from the tectonic plates of Iberia, Africa, Arabia, Iran, Eurasia, North Pacific, and North America (e.g., Haq, 2014). Extensive literature exists on this topic (e.g., Röhl and Ogg, 1998; Gréselle and Pittet, 2005; Rameil et al., 2012; Maurer et al., 2010, 2013; Horner et al., 2019; Ray et al., 2019). In Bover-Arnal et al. (2022), the discussion of the global significance of the Aptian relative sea-level fluctuations recorded in the Galve and Morella sub-basins (Fig. 1B–C) was focused on the coeval records of the North Cantabrian Basin (Iberian Plate), the Shu'aiba Formation (eastern Arabian Plate), as well as of the Matese Mountains, the Sorrento Peninsula and the Vocontian Basin (Euroasian Plate). In the present paper, this discussion is revised and extended to include also the African, Iranian and Pacific plates (Fig. 13).

Such remarkable examples of late early and/or early late Aptian major sea-level swings recorded in other basins worldwide showing marked similarity to the sedimentary results observed in the Maestrat Basin include south Tunisia (African Plate), where Hfaiedh et al. (2013) identified two subaerial exposure surfaces that were interpreted as major sequence boundaries (Fig. 13) and are time-coincident with the upper lower and lower upper Aptian subaerial unconformities in the Maestrat Basin (Fig. 2). In central Tunisia, similar third-order regressive events topped by discontinuity surfaces close to the boundaries between the early Aptian and late Aptian, and the *Epicheloniceras martini* and *Parahoplites melchioris* ammonite zones have been also documented by Ben Chaabane et al. (2019, 2021) (Fig. 13). In western Morocco, an upper lower Aptian, but slightly older (intra *Deshayesites deshayesi* Zone) major discontinuity surface exhibiting palaeokarst features was recorded in the Essaouira–Agadir Basin (Jaillard et al., 2019; Giraud et al., 2020).

Mehrabi et al. (2018) reported two subaerial unconformities capping the regressive Lower and Upper Carbonate members of the Dariyan Formation in offshore south-west Iran (Arabian Plate) (Fig. 13). The emersion surface capping the Lower Carbonate Member is of mid Aptian age and is overlain by transgressive basinal marls of the Kazhdumi Tongue Member, whereas the subaerial unconformity found at the top of the Upper Carbonate Member is late Aptian in age. This last emersion surface was also buried by early transgressive marls and limestones (Mehrabi et al., 2018).

On the eastern Arabian Plate, after major sea-level drop in the early late Aptian, and during a subsequent late Aptian lowstand stage, a carbonate platform also belonging to the Shu'aiba Formation developed basinwards and prograded into the Bab Basin (van Buchem et al., 2010; Maurer et al., 2010, 2013). In the platform-to-basin transition area of Las Mingachas (Fig. 1C) (Bover-Arnal et al., 2009, 2022), as well as in La Mola d'en Camaràs and La Mola de la Garumba (Morella Sub-basin) (Fig. 1B) (Bover-Arnal et al., 2014, 2022), lowstand prograding platforms also flourished basinwards and topographically below the margins of subaerially exposed highstand platforms. However, the age of the lowstand platforms developed in Las Mingachas and in the Morella Sub-basin is latest early Aptian (Fig. 2), whereas the lowstand platform described from the eastern Arabian Plate has been dated as late Aptian (van Buchem et al., 2010; Maurer et al., 2010, 2013). In addition, because of a rapid sea-level fall, which according to Maurer et al. (2013) occurred around the boundary between the *Epicheloniceras martini* and *Parahoplites melchioris* ammonite zones, and the following late Aptian lowstand phase, an incised valley system developed cutting into the top Shu'aiba Formation in offshore Qatar (Raven et al., 2010; Maurer et al., 2013) (Fig. 13). The valley incision is up to 8 km wide and between 50 and 65 m deep and exhibits strath terraces and an uppermost Aptian–Albian tidally-influenced siliciclastic infill (Raven et al., 2010; Maurer et al., 2013). On the other hand, the early late Aptian subaerial unconformity and associated valley incision documented in La Mola d'en Camaràs (Morella Sub-basin) (Fig. 1B) (Bover-Arnal et al., 2014, 2022) formed within the upper part of the *Epicheloniceras martini* Zone, very close to the boundary with the overlying *Parahoplites melchioris* Zone. This roughly time-equivalent incised valley development reported from the Maestrat Basin is >2 km wide and significantly deeper (≥115 m), and also exhibits strath terraces and a valley fill influenced by tides (see Bover-Arnal et al., 2014). However, the valley fill of the incision present in La Mola d'en Camaràs is younger and correlates with the upper part of the *Epicheloniceras*

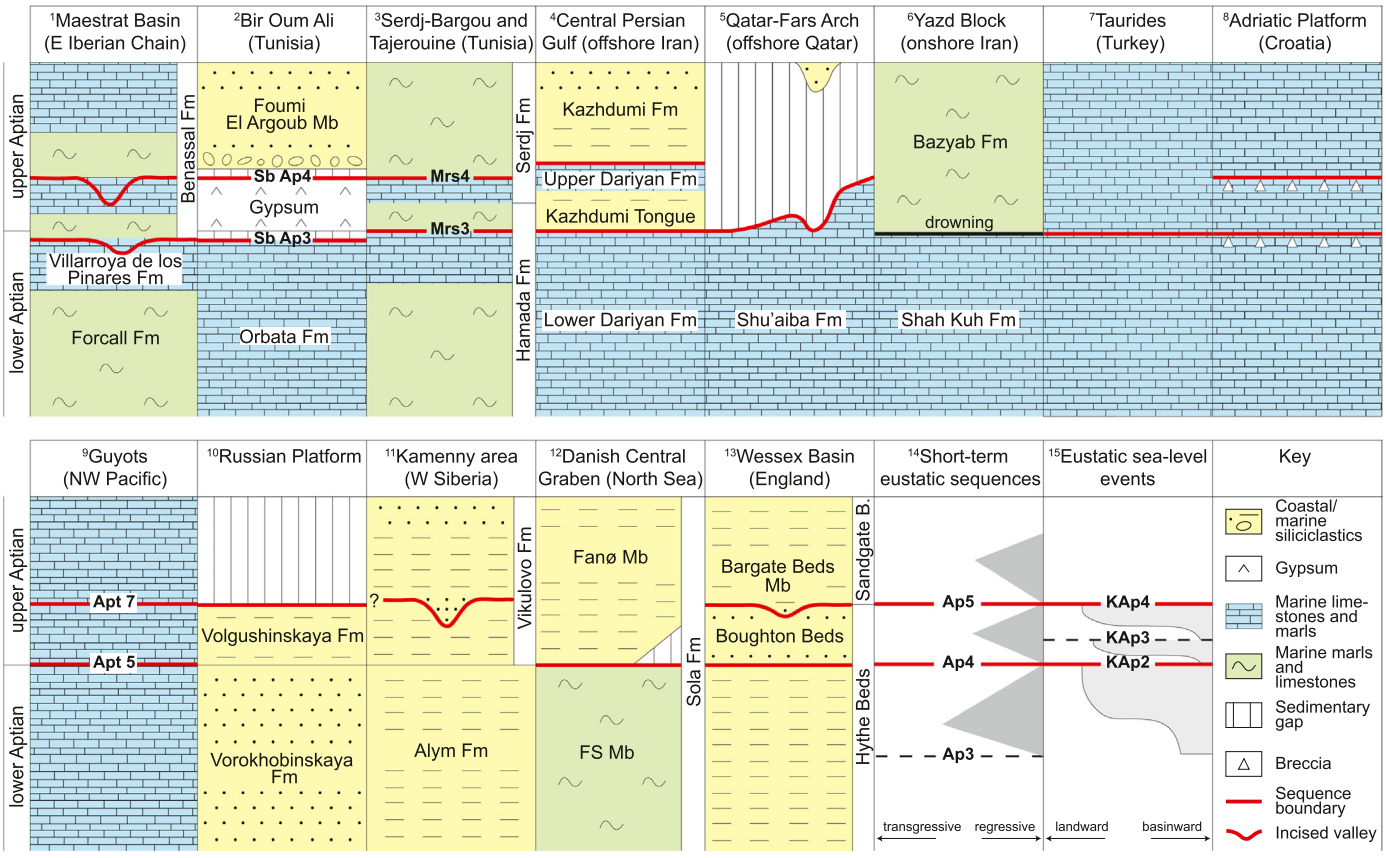

Fig. 13. Stratigraphic correlation of different locations displaying geological evidence of major regressions of relative sea-level and sequence boundaries, which may locally exhibit incised valleys, during the early Aptian (including the early/late Aptian boundary) and the late Aptian. The short-term eustatic transgressive–regressive sequences of Hardenbol et al. (1998) and the eustatic sea-level events found in Haq (2014) are also included in the correlation. The rather coeval occurrence of major relative sea-level falls and rises across various tectonic plates, such as Iberia, Eurasia, Arabia, Africa, and the Pacific, provides robust support for eustatic controls during the Aptian Stage. The data utilised for this correlation are drawn from [1]this study and Bover-Arnal et al. (2009, 2015, 2016, 2022); [2]Hfaiedh et al. (2013); [3]Ben Chaabane et al. (2019); [4]Mehrabi et al. (2018); [5]Raven et al. (2010) and Maurer et al. (2013); [6]Wilmsen et al. (2015); [7]Yilmaz and Altiner (2006); [8]Husinec et al. (2012); [9]Röhl and Ogg (1998); [10]Sahagian et al. (1996), Zorina and Ruban (2012) and Zorina (2014, 2016); [11]Medvedev et al. (2011); [12]van Buchem et al. (2018); [13]Ruffell and Wach (1991); [14]Hardenbol et al. (1998); and [15]Haq (2014).

martini and lowermost *Parahoplites melchioris* ammonoid biozones (Bover-Arnal et al., 2016). Hence, after the early late Aptian major fall in sea level recorded in the northern and southern margins of the Tethys, a subsequent rapid transgression occurred in the Maestrat Basin, which is not recorded in the eastern Arabian Plate.

In onshore western Central Iran (Iranian Plate), Wilmsen et al. (2015) identified a late early Aptian drowning surface recorded at the top of the rudist-bearing platform carbonates of the Shah Kuh Formation (Fig. 13). These platform limestones were buried by transgressive basinal marls and limestones with ammonites of the Bazyab Formation coinciding with the limit between the early Aptian and late Aptian (Wilmsen et al., 2015). Upon the Eurasian Plate, subaerial exposure surfaces capping upper lower Aptian platform carbonates were reported from southwest Turkey (Yilmaz and Altiner, 2006) (Fig. 13).

In the Aptian succession of the Adriatic Platform of Croatia, Husinec et al. (2012) identified five third-order sequence boundaries corresponding to major disconformities. One of these sequence boundaries is late early Aptian in age and caps regressive platform carbonates and breccia deposits, which formed as a result of subaerial exposure. This upper lower Aptian subaerial unconformity reported from Croatia seems to be time-equivalent to the deeply incised disconformity affecting the top of the Villarroya de los Pinares Formation in the Maestrat Basin (Figs. 2–4, 13). Moreover, in the lower upper Aptian record of the Adriatic Platform, Husinec et al. (2012) discussed an overall regressive succession of platform carbonates that is punctuated by two major subaerial disconformities, which also cap breccia deposits in proximal platform settings. This lower upper Aptian limestone succession exhibiting two major surfaces of emersion described by Husinec et al. (2012) is coeval with the subaerially exposed (Figs. 9–12), and locally incised (Bover-Arnal et al., 2014, 2022), highstand rudist-bearing carbonates of the lower part of the Benassal Formation studied (Figs. 2, 13). The three remaining third-order sequence boundaries that were identified by Husinec et al. (2012) in Croatia might not have equivalents in the Maestrat Basin, or these might correspond to maximum regressive surfaces that were interpreted as lower-order stratigraphic surfaces.

Upon the Pacific Plate, twelve surfaces of emersion were identified by Röhl and Ogg (1998) in the Aptian record of the Pacific Guyots. A major emergence episode of early Aptian age corresponding to sequence boundary 'Apt2' in Röhl and Ogg (1998) was correlated by these authors with a late early Aptian sea-level drop, which deeply incised the carbonate platforms flanking the Vocontian Basin (see e.g., Arnaud and Arnaud-Vanneau, 1990; Hunt and Tucker, 1993; Adatte et al., 2005). However, more recent studies based on ammonite biostratigraphy have reassigned as uppermost Barremian this major subaerial unconformity topping the peri-Vocontian rudist-dominated carbonate platforms (e.g., Frau et al., 2018). Röhl and Ogg (1998) recognised a second major episode of sea-level drop 'Apt7' occurring in the early late Aptian, at the limit between the *Parahoplites nutfieldensis* (=*Parahoplites melchioris*) and *Cheloniceras martinoides* zones (=*Epicheloniceras martini*) (see Fig. 2). Around the early/late Aptian boundary, Röhl and Ogg (1998) identified a minor sequence boundary, 'Apt5' (Fig. 13). The rest of subaerial exposure surfaces recognised by Röhl and Ogg (1998) would either lack equivalents in

the Maestrat Basin or might align with maximum regressive surfaces of different hierarchical levels.

In non-carbonate platform successions of Aptian age such as those from the Russian Platform, North Sea Basin, Wessex Basin (southern England) or western Canada, sea-level falls and rises roughly contemporaneous to the ones described in the Maestrat Basin are also recognisable (Fig. 13). A long-term relative sea-level fall starting in the late early Aptian, with a peak around the early/late Aptian boundary, and continuing into the late Aptian was described from the Russian Platform (Sahagian et al., 1996; Zorina and Ruban, 2012; Zorina, 2014, 2016). According to the quantified eustatic curves of Sahagian et al. (1996), the peak of the late early Aptian sea-level drop coinciding with the *Tropaeum bowerbanki* ammonoid Zone, which is a Boreal equivalent to the Mediterranean *Dufrenoyia furcata* Zone, showed a c. 20 m drop in sea level. For the late Aptian sea-level drop, Sahagian et al. (1996) give a tentative amplitude of c. 50 m. In this regard, Medvedev et al. (2011) documented incised valleys with depths attaining up to 90 m in the upper Aptian sedimentary record of western Siberia. The upper lower Aptian succession of the North Sea Basin is characterised by regressive marl and chalk deposits, which are capped by a sequence boundary, locally erosional, and interpreted as the result of a major fall in sea level (van Buchem et al., 2018). According to these authors, this sea-level drop exposed and eroded the margin of the basin. The age of the sequence boundary is correlatable with the top of the *Tropaeum bowerbanki* ammonoid Zone of the Boreal realm, and has been dated as latest early–earliest late Aptian (van Buchem et al., 2018).

The Aptian succession of the Isle of Wight (Wessex Basin; southern England) recorded a sedimentary gap and likely an associated sequence boundary within the Hythe Beds stratigraphic unit around the limit between the *Tropaeum bowerbanki* and *Cheloniceras martinoides* ammonite Boreal zones (Casey, 1961; Ruffell and Wach, 1991), which would be correlatable with the Mediterranean *Dufrenoyia furcata* and *Epicheloniceras martini* zones (Reboulet et al., 2018). Further within the sedimentary succession of the Isle of Wight, a lower upper Aptian sequence boundary, indicating a significant sedimentary hiatus, separates the Hythe Beds from the Sandgate Beds stratigraphic units. The latter surface was interpreted by Ruffell and Wach (1991) as an incised valley (Fig. 13). This regression event was identified around the limit between the *Cheloniceras martinoides* and *Parahoplites nutfieldiensis* ammonite Boreal zones, as outlined in the works of Casey (1961) and Ruffell and Wach (1991). These zones correspond in time to the *Epicheloniceras martini* and *Parahoplites melchioris* Mediterranean ammonite zones (Reboulet et al., 2018). In North America, the Aptian McMurray Formation (western Canada) contains incised-valley networks with troughs that locally show depths of ≥70 m (Horner et al., 2019).

Furthermore, the late early and early late Aptian drops in sea-level studied in the Maestrat Basin are correlatable with the major and medium sequence boundaries Ap4 and Ap5, respectively, of Hardenbol et al. (1998) occurring within the *Dufrenoyia furcata* and *Epicheloniceras martini* ammonoid zones (Fig. 2). In Haq (2014), these sea-level falls correspond to global cycle boundaries KAp2 and KAp4, respectively (Fig. 13).

6. Conclusions

Sedimentary archives of two major relative sea-level drops of late early and early late Aptian age associated with local development of incised valleys and forced regressive wedges, previously described in only eight outcrops in the Maestrat Basin, have been identified in five further locations within this basin. These findings corroborate that these relative sea-level fluctuations had at least a basin-wide significance. Comparable and coeval sedimentary successions showing evidence of major relative sea-level fall and rise have been documented in other basins from other tectonic plates such as the African, Iranian, Arabian, Eurasian, Pacific and North America. Eustasy is thus interpreted as the common main cause for these changes in accommodation in the different basins.

The sedimentary records of relative sea-level drop characterised in the Maestrat Basin include locally incised subaerial unconformities. The new records of subsequent base-level rise analysed correspond to tidally-influenced high-energy carbonate deposits back-filling incised valleys or overlying exposure surfaces, and a reduced in extent detached coral-bearing carbonate platform stacked in a retrograding pattern. The two incisions studied herein were carved into upper lower Aptian highstand carbonate platforms dominated by rudists and corals of the Villarroya de los Pinares Formation and show depths of c. 10 and 80 m. Accordingly, the Aptian relative sea-level oscillations documented had amplitudes of several tens of metres. Incised valleys or smaller-scale incisions are local features. However, as documented in this paper, the records of relative sea-level drops can also be identified in areas where incision does not occur as karst remnants and/or sharp, or slightly erosive, stratigraphic surfaces overlain by deposits influenced by tidal processes.

The finding of new evidence of major Aptian relative sea-level fluctuations in different outcrops throughout the Maestrat Basin demonstrates that future investigations into this topic at a Tethys scale should include, but not be limited to, a comprehensive analysis of other underexplored Aptian platform carbonate successions from other sub-basins of the basin such as Oliete, Las Parras, La Salzadella, El Perelló, Penyagolosa and Cedramán.

Data availability

No data was used for the research described in the article.

Declaration of competing interest

The authors declare that they have no known competing financial interests or personal relationships that could have appeared to influence the work reported in this paper.

Acknowledgements

We would like to express our gratitude to Etienne Jaillard, an anonymous reviewer, and Editor Catherine Chagué for their valuable suggestions, corrections, and constructive criticism, which significantly enhanced the final version of the manuscript. We are also grateful to John J. G. Reijmer, Peter W. Skelton and Jean Borgomano for reviewing and improving earlier versions of the manuscript. This paper is a contribution to IBERINSULA (PID2020-113912GB-100) and was funded by MCIN/AEI/10.13039/501100011033 and the European Regional Development Fund (ERDF), as well as by the Grup de Recerca Reconegut per la Generalitat de Catalunya 2021 SGR-Cat 00349 "Geologia Sedimentària".

References

Adatte, T., Arnaud Vanneau, A., Arnaud, H., 2005. The Hauterivian-lower Aptian sequence stratigraphy from Jura platform to Vocontian Basin: a multidisciplinary approach/ Field-trip of the 7th International symposium on the Cretaceous (September 1-4, 2005); [organized by] Université Joseph Fournier, Grenoble 1 Université de Neuchâtel, UNINE (insu-00723810). https://hal-insu.archives-ouvertes.fr/insu-00723810.

Al-Husseini, M.I., 2013. Antarctica's glacio-eustatic signature in the Aptian and late Miocene–Holocene: implications for what drives sequence stratigraphy. GeoArabia 18, 17–52.

Arnaud, H., Arnaud-Vanneau, A., 1990. Hauterivian to Lower Aptian carbonate shelf sedimentation and sequence stratigraphy in the Jura and no rthern subalpine chains (southeastern France and Swiss Jura). In: Tucker, M.E., Wilson, J.L., Crevello, P.O., Sarg, J.R., Read, J.F. (Eds.), Carbonate Platforms. International Association of Sedimentologists, Special Publicationvol. 9, pp. 203–233.

Ben Chaabane, N., Khemiri, F., Soussi, M., Latil, J.L., Robert, E., Belhajtaher, I., 2019. Aptian–Lower Albian Serdj carbonate platform of the Tunisian Atlas: development, demise and petroleum implication. Marine and Petroleum Geology 101, 566–591.

Ben Chaabane, N., Khemiri, F., Soussi, M., Belhaj Taher, I., 2021. Late Aptian carbonate platform evolution and controls (south Tethys, Tunisia): response to sea-level oscillations, palaeo-environmental changes and climate. Facies 67, 26. https://doi.org/10.1007/s10347-021-00634-z.

Bonin, A., Pucéat, E., Vennin, E., Mattioli, E., Aurell, M., Joachimiski, M., Barbarin, N., Laffont, R., 2016. Cool episode and platform demise in the Early Aptian: new insights on the links between climate and carbonate production. Paleoceanography 31, 66–80.
Bover-Arnal, T., Salas, R., 2019. Geology of the 'Sénia stone' from Ulldecona, Catalonia (Aptian, Maestrat Basin, Iberian Chain) and its implications for regional stratigraphy. Cretaceous Research 96, 38–58.
Bover-Arnal, T., Salas, R., Moreno-Bedmar, J.A., Bitzer, K., 2009. Sequence stratigraphy and architecture of a late Early–Middle Aptian carbonate platform succession from the western Maestrat Basin (Iberian Chain, Spain). Sedimentary Geology 219, 280–301.
Bover-Arnal, T., Moreno-Bedmar, J.A., Salas, R., Skelton, P.W., Bitzer, K., Gili, E., 2010. Sedimentary evolution of an Aptian syn-rift carbonate system (Maestrat Basin, E Spain): effects of accommodation and environmental change. Geologica Acta 8, 249–280.
Bover-Arnal, T., Salas, R., Martín-Closas, C., Schlagintweit, F., Moreno-Bedmar, J.A., 2011. Expression of an oceanic anoxic event in a neritic setting: lower Aptian coral rubble deposits from the western Maestrat Basin (Iberian Chain, Spain). Palaios 26, 18–32.
Bover-Arnal, T., Löser, H., Moreno-Bedmar, J.A., Salas, R., Strasser, A., 2012. Corals on the slope (Aptian, Maestrat Basin, Spain). Cretaceous Research 37, 43–64.
Bover-Arnal, T., Salas, R., Guimerà, J., Moreno-Bedmar, J.A., 2014. Deep incision on an Aptian carbonate succession indicates major sea-level fall in the Cretaceous. Sedimentology 61, 1558–1593.
Bover-Arnal, T., Pascual-Cebrian, E., Skelton, P.W., Gili, E., Salas, R., 2015. Patterns in the distribution of Aptian rudists and corals within a sequence-stratigraphic framework (Maestrat Basin, E Spain). Sedimentary Geology 321, 86–104.
Bover-Arnal, T., Moreno-Bedmar, J.A., Frijia, G., Pascual-Cebrian, E., Salas, R., 2016. Chronostratigraphy of the Barremian–Early Albian of the Maestrat Basin (E Iberian Peninsula): integrating strontium-isotope stratigraphy and ammonoid biostratigraphy. Newsletters on Stratigraphy 49, 41–68.
Bover-Arnal, T., Salas, R., Guimerà, J., Moreno-Bedmar, J.A., 2022. Eustasy in the Aptian world: a vision from the eastern margin of the Iberian Plate. Global and Planetary Change 214, 103849. https://doi.org/10.1016/j.gloplacha.2022.103849.
Canérot, J., Crespo, A., Navarro, D., 1979. Montalbán, hoja n° 518. Mapa Geológico de España 1:50.000. 2ª Serie. 1ª Edición. Servicio de Publicaciones, Ministerio de Industria y Energía, Madrid (31 pp., in Spanish).
Canérot, J., Cugny, P., Pardo, G., Salas, R., Villena, J., 1982. Ibérica Central-Maestrazgo. In: García, A. (Ed.), El Cretácico de España. Universidad Complutense de Madrid, pp. 273–344 (in Spanish).
Casey, R., 1961. The stratigraphical palaeontology of the Lower Greensand. Palaeontology 3, 487–622.
Catuneanu, O., Abreu, V., Bhattacharya, J.P., Blum, M.D., Dalrymple, R.W., Eriksson, P.G., Fielding, C.R., Fisher, W.L., Galloway, W.E., Gibling, M.R., Giles, K.A., Holbrook, J.M., Jordan, R., Kendall, C.G.St.C., Macurda, B., Martinsen, O.J., Miall, A.D., Neal, J.E., Nummedal, D., Pomar, L., Posamentier, H.W., Pratt, B.R., Sarg, J.F., Shanley, K.W., Steel, R.J., Strasser, A., Tucker, M.E., Winker, C., 2009. Towards the standardization of sequence stratigraphy. Earth-Science Reviews 92, 1–33.
Chaumillon, E., Proust, J.-N., Menier, D., Weber, N., 2008. Incised-valley morphologies and sedimentary-fills within the inner shelf of the Bay of Biscay (France): a synthesis. Journal of Marine Systems 72, 383–396.
Cherchi, A., Schroeder, R., 2013. The *Praeorbitolina/Palorbitolinoides* Association: an Aptian biostratigraphic key-interval at the southern margin of the Neo-Tethys. Cretaceous Research 39, 70–77.
Cors, J., Heimhofer, U., Adatte, T., Hochuli, P.A., Huck, S., Bover-Arnal, T., 2015. Spore-pollen assemblages show delayed terrestrial cooling in the aftermath of OAE 1a. Geological Magazine 152, 632–647.
Dalrymple, R.W., Zaitlin, B.A., Boyd, R., 1992. Estuarine facies models: conceptual basis and stratigraphic implications. Journal of Sedimentary Petrology 62, 1130–1146.
Davies, A., Gréselle, B., Hunter, S.J., Baines, G., Robson, C., Haywood, A.M., Ray, D.C., Simmons, M.D., van Buchem, F.S.P., 2020. Assessing the impact of aquifer-eustasy on short-term Cretaceous sea-level. Cretaceous Research 112, 104445. https://doi.org/10.1016/j.cretres.2020.104445.
Dunham, R.J., 1962. Classification of carbonate rocks according to depositional texture. In: Ham, W.E. (Ed.), Classification of Carbonate Rocks American Association of Petroleum Geologists Memoirevol. 1, pp. 108–121.
Dutton, A., Villa, A., Chutcharavan, P.M., 2022. Compilation of Last Interglacial (Marine Isotope Stage 5e) sea-level indicators in the Bahamas, Turks and Caicos, and the east coast of Florida, USA. Earth System Science Data 14, 2385–2399.
Dyer, B., Austermann, J., D'Andrea, W.J., Creel, R.C., Sandstrom, M.R., Cashman, M., Rovere, A., Raymo, M.E., 2021. Sea-level trends across The Bahamas constrain peak last interglacial ice melt. Proceedings of the National Academy of Sciences 118, e2026839118. https://doi.org/10.1073/pnas.2026839118.
Eberli, G.P., Ginsburg, R.N., 1987. Segmentation and coalescence of Cenozoic carbonate platforms, northwestern Great Bahama Bank. Geology 15, 75–79.
Embry, A.F., Klovan, J.E., 1971. A Late Devonian reef tract on northeastern Banks Island, N.W.T. Bulletin of Canadian Petroleum Geology 19, 730–781.
Embry, J.-C., Vennin, E., van Buchem, F.S.P., Schroeder, R., Pierre, C., Aurell, M., 2010. Sequence stratigraphy and carbon isotope stratigraphy of an Aptian mixed carbonate-siliciclastic platform to basin transition (Galve sub-basin, NE Spain). In: van Buchem, F.S.P., Ger des, K.D., Esteban, M. (Eds.), Mesozoic and Cenozoic Carbonate Systems of the Mediterranean and the Middle East: Stratigraphic and Diagenetic Reference Models. Geological Society, London, Special Publicationsvol. 329, pp. 113–143.
Frau, C., Anthony, J.-B.T., Lanteaume, C., Masse, J.-P., Pictet, A., Bulot, L.G., Luber, T.L., Redfern, J., Borgomano, J.R., Léonide, P., Fournier, F., Massonnat, G., 2018. Late Barremian–early Aptian ammonite bioevents from the Urgonian-type series of Provence, southeast France: regional stratigraphic correlations and implications for dating the peri-Vocontian carbonate platforms. Cretaceous Research 90, 222–253.
Garcia, R., Moreno-Bedmar, J.A., Bover-Arnal, T., Company, M., Salas, R., Latil, J.L., Martín-Martín, J.D., Gomez-Rivas, E., Bulot, L.G., Delanoy, G., Martínez, R., Grauges, A., 2014. Lower Cretaceous (Hauterivian–Albian) ammonite biostratigraphy in the Maestrat Basin (E Spain). Journal of Iberian Geology 40, 99–112.
García-Senz, J., Salas, R., 2011. Sedimentary response to continental rifting in Iberia. In: Bádenas, B., Aurell, M., Alonso-Zarza, A.M. (Eds.), Abstracts, 28th IAS Meeting of Sedimentology, Zaragoza, Spain. IAS, p. 31.
Gautier, F., 1980. Villarluengo, hoja n° 543. Mapa Geológico de España 1:50.000. 2ª Serie. 1ª Edición. Servicio de Publicaciones, Ministerio de Industria y Energía, Madrid (45 pp., in Spanish).
Giraud, F., Kassab, W.H., Robert, E., Jaillard, E., Spangenberg, J.E., Masrour, M., Hammed, M.S., Aly, M.F., El Hariri, K., 2020. Integrated stratigraphy of the latest Barremian–early Albian interval in the western part of the Tethyan margin: new data from the Essaouira–Agadir Basin (Western Morocco). Newsletters on Stratigraphy 54, 43–78.
Goldsworthy, M., Jackson, J., 2000. Active normal fault evolution in Greece revealed by geomorphology and drainage patterns. Journal of the Geological Society, London 157, 967–981.
Gréselle, B., Pittet, B., 2005. Fringing carbonate platforms at the Arabian Plate margin in northern Oman during the Late Aptian–Middle Albian: evidence for high-amplitude sea-level changes. Sedimentary Geology 175, 367–390.
Guimerà, J., 1994. Cenozoic evolution of eastern Iberia: structural data and dynamic model. Acta Geologica Hispánica 29, 57–66.
Guimerà, J., 2018. Structure of an intraplate fold-and-thrust belt: the Iberian Chain. A synthesis. Geologica Acta 16, 427–438.
Haq, B.U., 2014. Cretaceous eustasy revisited. Global and Planetary Change 113, 44–58.
Hardenbol, J., Thierry, J., Farley, M.B., Jacquin, T., de Graciansky, P.-C., Vail, P.R., 1998. Mesozoic and Cenozoic sequence chronostratigraphic framework of European basins. In: de Graciansky, P.-C., Hardenbol, J., Jacquin, T., Vail, P.R. (Eds.), Mesozoic and Cenozoic Sequence Stratigraphy of European Basins. Society of Economic Paleontologists and Mineralogists Special Publicationvol. 60, pp. 3–13.
Heimhofer, U., Adatte, T., Hochuli, P.A., Burla, S., Weissert, H., 2008. Coastal sediments from the Algarve: low-latitude climate archive for the Aptian-Albian. International Journal of Earth Sciences 97, 785–797.
Hfaiedh, R., Arnaud Vanneau, A., Godet, A., Arnaud, H., Zghal, I., Ouali, J., Latil, J.-L., Jallali, H., 2013. Biostratigraphy and palaeoenvironmental evolution of the Aptian succession at Jebel Bir Oum Ali (Northern Chain of Chotts, South Tunisia). Cretaceous Research 46, 177–207.
Horner, S.C., Hubbard, S.M., Martin, H.K., Hagstrom, C.A., Leckie, D.A., 2019. The impact of Aptian glacio-eustasy on the stratigraphic architecture of the Athabasca Oil Sands, Alberta, Canada. Sedimentology 66, 1600–1642.
Horozal, S., Chae, S., Seo, J.M., Lee, S.M., Han, H.S., Cukur, D., Kim, E.D., Son, J.H., 2021. Quaternary evolution of the southeastern Korean continental shelf, East Sea: paleo-incised valley and channel systems. Marine and Petroleum Geology 128, 105011. https://doi.org/10.1016/j.marpetgeo.2021.105011.
Hunt, D., Tucker, M.E., 1993. Sequence stratigraphy of carbonate shelves with an example from the mid-Cretaceous (Urgonian) of southeast France. In: Posamentier, H.W., Summerhayes, C.P., Haq, B.U., Allen, G.P. (Eds.), Sequence Stratigraphy and Facies Associations. International Association of Sedimentologists, Special Publicationvol. 18, pp. 307–341.
Husinec, A., Harman, C.A., Regan, S.P., Mosher, D.A., Sweeney, R.J., Read, J.F., 2012. Sequence development influenced by intermittent cooling events in the Cretaceous Aptian greenhouse, Adriatic platform, Croatia. American Association of Petroleum Geologists Bulletin 96, 2215–2244.
Immenhauser, A., 2005. High-rate sea-level change during the Mesozoic: new approaches to an old problem. Sedimentary Geology 175, 277–296.
Jaillard, E., Kassab, W.H., Giraud, F., Robert, E., Masrour, M., Bouchaou, L., El Hariri, K., Hammed, M.S., Aly, M.F., 2019. Aptian–early Albian sedimentation in the Essaouira–Agadir basin, Western Morocco. Cretaceous Research 102, 59–80.
Loma-Villacorta, R., García-Gómez, M., Díez-Masip, J., 2022. Controlling factors on a Berriasian-Barremian isolated carbonate platform in central Porcupine Basin, SW Ireland. European Association of Geoscientists & Engineers, Conference Proceedings, 83rd EAGE Annual Conference & Exhibition 2022, pp. 1–5 https://doi.org/10.3997/2214-4609.202210990.
Martín-Chivelet, J., López-Gómez, J., Aguado, R., Arias, C., Arribas, J., Arribas, M.E., Aurell, M., Bádenas, B., Benito, M.I., Bover-Arnal, T., Casas-Sainz, A., Castro, J.M., Coruña, F., de Gea, G.A., Fornós, J.J., Fregenal-Martínez, M., García-Senz, J., Garófano, D., Gelabert, B., Giménez, J., González-Acebrón, J., Guimerà, J., Liesa, C.L., Mas, R., Meléndez, N., Molina, J.M., Muñoz, J.A., Navarrete, R., Nebot, M., Nieto, L.M., Omodeo-Salé, S., Pedrera, A., Peropadre, C., Quijada, I.E., Quijano, M.L., Reolid, M., Robador, A., Rodríguez-López, J.P., Rodríguez-Perea, A., Rosales, I., Ruiz-Ortiz, P.A., Sàbat, F., Salas, R., Soria, A.R., Suarez-Gonzalez, P., Vilas, L., 2019. The Late Jurassic–Early Cretaceous rifting. In: Quesada, C., Oliveira, J.T. (Eds.), The Geology of Iberia: A Geodynamic Approach. The Alpine Cyclevol. 3. Springer, Heidelberg, pp. 60–63. https://doi.org/10.1007/978-3-030-11295-0.
Martín-Martín, J.D., Gomez-Rivas, E., Bover-Arnal, T., Travé, A., Salas, R., Moreno-Bedmar, J.A., Tomás, S., Corbella, M., Teixell, A., Vergés, J., Stafford, S.L., 2013. The Upper Aptian to Lower Albian synrift carbonate succession of the southern Maestrat Basin (Spain): facies architecture and fault-controlled stratabound dolostones. Cretaceous Research 41, 217–236.
Maurer, F., Al-Mehsin, K., Pierson, B.J., Eberli, G.P., Warrlich, G., Drysdale, D., Droste, H.J., 2010. Facies characteristics and architecture of Upper Aptian Shu'aiba clinoforms in Abu Dhabi. In: van Buchem, F.S.P., Al-Husseini, M.I., Maurer, F. , Droste, H.J. (Eds.), Barremian–Aptian Stratigraphy and Hydrocarbon Habitat of the Eastern Arabian Plate. GeoArabia Special Publication 4vol. 2. Gulf PetroLink, Bahrain, pp. 445–468.
Maurer, F., van Buchem, F.S.P., Eberli, G.P., Pierson, B.J., Raven, M.J., Larsen, P.-H., Al-Husseini, M.I., Vincent, B., 2013. Late Aptian long-lived glacio-eustatic lowstand recorded on the Arabian Plate. Terra Nova 25, 87–94.

McClung, W.S., Cuffey, C.A., Eriksson, K.A., Terry Jr., D.O., 2016. An incised valley fill and lowstand wedges in the Upper Devonian Foreknobs Formation, central Appalachian Basin: implications for Famennian glacioeustasy. Palaeogeography, Palaeoclimatology, Palaeoecology 446, 125–143.
Medvedev, A.L., Lopatin, A.Y., Masalkin, Y.V., 2011. Comparative characteristics of the lithological composition of the incised valley fill and host sediments of the Vikulovo Formation, Kamenny Area, West Siberia. Lithology and Mineral Resources 46, 369–381.
Mehrabi, H., Rahimpour-Bonab, H., Al-Aasm, I., Hajikazemi, E., Esrafili-Dizaji, B., Dalvand, M., Omidvar, M., 2018. Palaeo-exposure surfaces in the Aptian Dariyan Formation, offshore SW Iran: geochemistry and reservoir implications. Journal of Petroleum Geology 41, 467–494.
Miller, K.G., Kominz, M.A., Browning, J.V., Wright, J.D., Mountain, G.S., Katz, M.E., Sugarman, P.J., Cramer, B.S., Christie-Blick, N., Pekar, S.F., 2005. The Phanerozoic record of global sea-level change. Science 310, 1293–1298.
Moreno-Bedmar, J.A., Company, M., Bover-Arnal, T., Salas, R., Delanoy, G., Martínez, R., Grauges, A., 2009. Biostratigraphic characterization by means of ammonoids of the lower Aptian Oceanic Anoxic Event (OAE 1a) in the eastern Iberian Chain (Maestrat Basin, eastern Spain). Cretaceous Research 30, 864–872.
Moreno-Bedmar, J.A., Company, M., Bover-Arnal, T., Salas, R., Maurrasse, F.J., Delanoy, G., Grauges, A., Martínez, R., 2010. Lower Aptian ammonite biostratigraphy in the Maestrat Basin (Eastern Iberian Chain, Eastern Spain). A Tethyan transgressive record enhanced by synrift subsidence. Geologica Acta 8, 281–299.
Núñez-Useche, F., Barragán, R., Torres-Martínez, M.A., López-Zúñiga, P.A., Moreno-Bedmar, J.A., Chávez-Cabello, G., Canet, C., Chacón-Baca, E., 2020. Response of the western proto-North Atlantic margin to the early Aptian oceanic anoxic event (OAE) 1a: an example from the Cupido platform margin-Gulf of Mexico, NE Mexico. Cretaceous Research 113, 104488.
O'Sullivan, J.M., Jones, S.M., Hardy, R.J., 2009. Controls on the Lower Cretaceous carbonate habitats of the South Porcupine and Goban Spur Basins, Offshore Ireland. SPE Offshore Europe Oil and Gas Conference and Exhibition, Aberdeen, UK, September 2009, SPE-125056-MS https://doi.org/10.2118/125056-MS.
Pascual-Cebrian, E., Götz, S., Bover-Arnal, T., Skelton, P.W., Gili, E., Salas, R., Stinnesbeck, W., 2016. Calcite/aragonite ratio fluctuations in Aptian rudist bivalves: correlation with changing temperatures. Geology 44, 135–138.
Pellen, R., Aslanian, D., Rabineau, M., Suc, J.P., Gorini, C., Leroux, E., Blanpied, C., Silenziario, C., Popescu, S.M., Rubino, J.L., 2019. The Messinian Ebro River incision. Global and Planetary Change 181, 102988. https://doi.org/10.1016/j.gloplacha.2019.102988.
Peropadre Medina, C., 2012. El Aptiense del margen occidental de la Cuenca del Maestrazgo: controles tectónico, eustático y climático en la sedimentación. Universidad Complutense de Madrid (PhD thesis, 649 pp., in Spanish).
Phelps, R.M., Kerans, C., Da-Gama, R.O.B.P., Jeremiah, J., Hull, D., Loucks, R.G., 2015. Response and recovery of the Comanche carbonate platform surrounding multiple Cretaceous oceanic anoxic events, northern Gulf of Mexico. Cretaceous Research 54, 117–144.
Pictet, A., Delanoy, G., Adatte, T., Spangenberg, J.E., Baudouin, C., Boselli, P., Boselli, M., Kindler, P., Föllmi, K.B., 2015. Three successive phases of platform demise during the early Aptian and their association with the oceanic anoxic Selli episode (Ardèche, France). Palaeogeography, Palaeoclimatology, Palaeoecology 418, 101–125.
Pittet, B., van Buchem, F.S.P., Hillgärtner, H., Razin, P., Grötsch, J., Droste, H., 2002. Ecological succession, palaeoenvironmental change, and depositional sequences of Barremian–Aptian shallow-water carbonates in northern Oman. Sedimentology 49, 555–581.
Posenato, R., Morsili, M., Guerzoni, S., Bassi, D., 2018. Palaeoecology of *Chondrodonta* (Bivalvia) from the lower Aptian (Cretaceous) Apulia Carbonate Platform (Gargano Promontory, southern Italy). Palaeogeography, Palaeoclimatology, Palaeoecology 508, 188–201.
Rameil, N., Immenhauser, A., Csoma, A.É., Warrlich, G., 2012. Surfaces with a long history: the Aptian top Shu'aiba Formation unconformity, Sultanate of Oman. Sedimentology 59, 212–248.
Raven, M.J., van Buchem, F.S.P., Larsen, P.-H., Surlyk, F., Steinhardt, H., Cross, D., Klem, N., Emang, M., 2010. Late Aptian incised valleys and siliciclastic infill at the top of the Shu'aiba Formation (Block 5, offshore Qatar). In: van Buc hem, F.S.P., Al-Husseini, M.I., Maurer, F., Droste, H.J. (Eds.), Barremian–Aptian Stratigraphy and Hydrocarbon Habitat of the Eastern Arabian Plate. GeoArabia Special Publication 4vol. 2. Gulf PetroLink, Bahrain, pp. 469–502.
Ray, D.C., van Buchem, F.S.P., Baines, G., Davies, A., Gréselle, B., Simmons, M.D., Robson, C., 2019. The magnitude and cause of short-term eustatic Cretaceous sea-level change: a synthesis. Earth-Science Reviews 197, 102901. https://doi.org/10.1016/j.earscirev.2019.102901.
Reboulet, S., Szives, O., Aguirre-Urreta, B., Barragán, R., Company, M., Frau, C., Kakabadze, M.V., Klein, J., Moreno-Bedmar, J.A., Lukeneder, A., Pictet, A., Ploch, I., Raisossadat, S.N., Vasícek, Z., Baraboshkin, E.J., Mitta, V.V., 2018. Report on the 6th International Meeting of the IUGS Lower Cretaceous Ammonite Working Group, the Kilian Group (Vienna, Austria, 20th August 2017). Cretaceous Research 91, 100–110.
Röhl, U., Ogg, J.G., 1998. Aptian–Albian eustatic sea-levels. In: Camoin, G.F., Davies, P.J. (Eds.), Reefs and Carbonate Pl atforms in the Pacific and Indian Oceans. International Association of Sedimentologists, Special Publicationsvol. 25, pp. 93–136.
Ruberti, D., Bravi, S., Carannante, G., Vigorito, M., Simone, L., 2013. Decline and recovery of the Aptian carbonate factory in the southern Apennine carbonate shelves (southern Italy): climatic/oceanographic vs. local tectonic controls. Cretaceous Research 39, 112–132.
Ruffell, A.H., Wach, G.D., 1991. Sequence stratigraphic analysis of the Aptian–Albian Lower Greensand in southern England. Marine and Petroleum Geology 8, 341–353.
Sahagian, D., Pinous, O., Olferiev, A., Zakharov, V., 1996. Eustatic curve for the Middle Jurassic–Cretaceous based on Russian Platform and Siberian stratigraphy: zonal resolution. American Association of Petroleum Geologists Bulletin 80, 1433–1458.
Salas, R., 1987. El Malm i el Cretaci inferior entre el Massís de Garraf i la Serra d'Espadà. Anàlisi de Conca. Universitat de Barcelona (PhD thesis, 541 pp., in Catalan) http://hdl.handle.net/10803/669675.
Salas, R., Guimerà, J., Mas, R., Martín-Closas, C., Menéndez, A., Alonso, A., 2001. Evolution of the Mesozoic Central Iberian Rift System and its Cainozoic inversion (Iberian Chain). In: Ziegler, P.A., Cavazza, W., Roberston, A.H.F., Crasquin-Soleau, S. (Eds.), Peri-Tethys Memoir 6: Peri-Tethyan Rift/Wrench Basins and Passive Margins. vol. 186. Memoires du Museum National d'Histoire Naturelle, Paris, pp. 145–186.
Salas, R., García-Senz, J., Guimerà, J., Bover-Arnal, T., 2010. Opening of the Atlantic and development of the Iberian intraplate rift basins during the late Jurassic–early Cretaceous. In: Pena dos Reis, R., Pimentel, N. (Eds.), II Central & North Atlantic conjugate margins conference, Lisbon 2010. Rediscovering the Atlantic: New Ideas for an Old Sea. Extended Abstracts vol. 3. ISBN: 978-989-96923-1-2, pp. 245–248.
Schlagintweit, F., Bover-Arnal, T., 2013. Remarks on *Bacinella* Radoičić, 1959 (type species *B. irregularis*) and its representatives. Facies 59, 59–73.
Simón, J.L., Liesa, C.L., Soria, A.R., 1998. Un sistema de fallas normales sinsedimentarias en las unidades de facies Urgon de Aliaga. Geogaceta 24, 291–294 (in Spanish).
Sirna, G., 1999. Some Late Jurassic and Early Cretaceous nerineids from the Maestrat Basin, Spain. Geologica Romana 35, 35–43.
Skelton, P.W., Gili, E., 2012. Rudists and carbonate platforms in the Aptian: a case study on biotic interactions with ocean chemistry and climate. Sedimentology 59, 81–117.
Skelton, P.W., Gili, E., Bover-Arnal, T., Salas, R., Moreno-Bedmar, J.A., 2010. A new species of Polyconites from the uppermost Lower Aptian of Iberia and the early evolution of *Polyconitid* rudists. Turkish Journal of Earth Sciences 19, 557–572.
Skelton, P.W., Castro, J.M., Ruiz-Ortiz, P.A., 2019. Aptian carbonate platform development in the Southern Iberian Palaeomargin (Prebetic of Alicante, SE Spain). Bulletin de la Société Géologique de France - Earth Sciences Bulletin 190, 3. https://doi.org/10.1051/bsgf/2019001.
Skrivanek, A., Li, J., Dutton, A., 2018. Relative sea-level change during the Last Interglacial as recorded in Bahamian fossil reefs. Quaternary Science Reviews 200, 160–177.
Tomás, S., Löser, H., Salas, R., 2008. Low-light and nutrient-rich coral assemblages in an Upper Aptian carbonate platform of the southern Maestrat Basin (Iberian Chain, eastern Spain). Cretaceous Research 29, 509–534.
van Buchem, F.S.P., Al-Husseini, M.I., Maurer, F., Droste, H.J., Yose, L.A., 2010. Sequence-stratigraphic synthesis of the Barremian–Aptian of the eastern Arabian Plate and implications for the petroleum habitat. In: van Buchem, F.S.P., Al-Husseini, M.I., Maurer, F., Droste, H.J. (Eds.), Barremian–Aptian Stratigraphy and Hydrocarbon Habitat of the Eastern Arabian Plate. GeoArabia Special Publication 4vol. 1. Gulf PetroLink, Bahrain, pp. 9–48.
van Buchem, F.S.P., Smit, F.W.H., Buijs, G.J.A., Trudgill, B., Larsen, P.-H., 2018. Tectonostratigraphic framework and depositional history of the Cretaceous–Danian succession of the Danish Central Graben (North Sea) — new light on a mature area. Geological Society, London, Petroleum Geology Conference Series 8, 9–46.
Vennin, E., Aurell, M., 2001. Stratigraphie sequentielle de l'Aptien du sous-basin de Galvé (Province de Teruel, NE de l'Espagne). Bulletin de la Societe Geologique de France 172, 397–410 (in French with English abstract).
Wang, R., Colombera, L., Mountney, N.P., 2019. Geological controls on the geometry of incised-valley fills: insights from a global dataset of late-Quaternary examples. Sedimentology 66, 2134–2168.
Wilmsen, M., Fürsich, F.T., Majidifard, M.R., 2015. An overview of the Cretaceous stratigraphy and facies development of the Yazd Block, western Central Iran. Journal of Asian Earth Sciences 102, 73–91.
Winterer, E.L., 1991. The Tethyan Pacific during Late Jurassic and Cretaceous times. Palaeogeography, Palaeoclimatology, Palaeoecology 87, 253–265.
Ximenes Neto, A.R., Pessoa, P.R.S., Piheiro, L.S., Morais, J.O., 2021. Seismic stratigraphy of a partially filled incised valley on a semi-arid continental shelf, Northeast Brazil. Geo-Marine Letters 41, 18. https://doi.org/10.1007/s00367-021-00687-7.
Yao, S., Gomez-Rivas, E., Martín-Martín, J.D., Gómez-Gras, D., Travé, A., Griera, A., Howell, J.A., 2020. Fault-controlled dolostone geometries in a transgressive–regressive sequence stratigraphic framework. Sedimentology 67, 3290–3316.
Yilmaz, I.Ö., Altiner, D., 2006. Cyclic palaeokarst surfaces in Aptian peritidal carbonate successions (Taurides, southwest Turkey): internal structure and response to mid-Aptian sea-level fall. Cretaceous Research 27, 814–827.
Zorina, S.O., 2014. Eustatic, tectonic, and climatic signatures in the Lower Cretaceous siliciclastic succession on the Eastern Russian Platform. Palaeogeography, Palaeoclimatology, Palaeoecology 412, 91–98.
Zorina, S.O., 2016. Sea-level and climatic controls on Aptian depositional environments of the Eastern Russian Platform. Palaeogeography, Palaeoclimatology, Palaeoecology 441, 599–609.
Zorina, S.O., Ruban, D.A., 2012. Hauterivian-Aptian (Early Cretaceous) transgression-regression cycles on the eastern Russian Platform and their inter-regional correlation. GeoActa 11, 41–50.